Chapter 7

Chirped Fiber Bragg Gratings

"Chirp" is the high-pitched varying sound emitted by certain birds and bats. Gratings that have a nonuniform period along their length are therefore known as chirped. Chirp in gratings may take many different forms. The period may vary symmetrically, either increasing or decreasing in period around a pitch in the middle of a grating. The chirp may be linear, i.e., the period varies linearly with length of the grating [1], may be quadratic [2], or may even have jumps in the period [3]. A grating could also have a period that varies *randomly* along its length [4], over and above a general trend; for example, uniform, linear chirp. Chirp maybe imparted in several ways: by exposure to UV beams of nonuniform intensity of the fringe pattern, varying the refractive index along the length of a uniform period grating [5], altering the coupling constant κ_{ac} of the grating as a function of position [6], incorporating a chirp in the inscribed grating [7], fabricating gratings in a tapered fiber [8], applying of nonuniform strain [9] etc., many of which have been covered in Chapter 3. All these gratings have special characteristics, which are like signatures and may be recognized as special features of the type of grating. Chirped gratings have many applications. In particular, the linearly chirped grating has found a special place in optics: as a dispersion-correcting and compensating device. This application has also triggered the fabrication of ultralong, broad-bandwidth gratings of high quality, for high-bit-rate transmission in excess of 40 Gb/sec over 100 km [10] or more [11] and in WDM transmission [12]. Some of the other applications include chirped

pulse amplification [13], chirp compensation of gain-switched semiconductor lasers [14], sensing [15], higher-order fiber dispersion compensation [16], ASE suppression [17], amplifier gain flattening [18], and band-blocking and band-pass filters [19].

7.1 General characteristics of chirped gratings

It has been recognized for a long time that gratings can be used for correcting chromatic dispersion [20–22]. Winful [23] proposed the application of a fiber grating filter for the correction of nonlinear chirp to compress a pulse in transmission in a long grating. It was also suggested that since these gratings display negative group-velocity dispersion, their application in dispersion compensation could be tailored by chirping of the grating [23]. These are known as dispersion compensating gratings (DCGs). Nonlinear transmission is also a subject of renewed interest in long gratings [24–28]. Kuo *et al.* [29] measured the negative-group-velocity dispersion of Bragg gratings in the visible wavelength region. While the dispersion in these gratings in transmission is large, a limiting factor is the narrow bandwidth over which they can be used to correct for linear dispersion [30,31]. The drawback of such an arrangement is that the gratings have to be used on the edge of the band and consequently introduce a loss penalty, since some of the light is reflected, although it has been shown that strong, long, highly reflective gratings can be used to compensate for dispersion in communication links in transmission with negligible loss [32], by proper design of the grating. For high-bit-rate systems, higher-order dispersion effects become important, dissipating the advantage of the grating used in transmission. The criteria used for the design of the grating to compress pulses in a near ideal manner are a compromise between the reduction of higher-order dispersion and pulse recompression. Bandwidths are limited with this configuration by the strength of the coupling constant and length of a realizable uniform period grating. Uniform period DCGs may find applications in closely spaced WDM systems.

If the coupling constant κ_{ac} is ramped linearly as a function of grating length, the grating exhibits strong dispersion. Used in reflection, an 81-mm-long grating had a coupling coefficient that was varied from zero to 12 cm^{-1} to achieve a dispersion of ~3.94 nsec/nm [6] but over a bandwidth of only ~0.2 nm. These gratings typically have >99% in-band reflectivity.

Despite the large dispersion, unchirped gratings have symmetrical delay characteristics, so that the dispersion changes sign when detuning from one side of the bandgap to the other [33]. With the several possibilities of using unchirped gratings for the management of dispersion, chirped gratings are even more attractive for this application, despite their use in reflection.

The application of reflective chirped gratings for dispersion compensation was originally suggested by Ouellette [34]. The group delay through a fiber is large in comparison with the dispersion of standard optical fibers at 1550 nm. A grating reflecting a band of wavelengths distributed over its length benefits from the large group delay in the fiber. We now assess the performance of chirped gratings as a dispersive filter specifically for the compensation of chromatic dispersion.

Figure 7.1 shows a schematic of a chirped grating, of length L_g and chirped bandwidth $\Delta\lambda_{\text{chirp}}$. Referring to Fig. 7.1, we note that the chirp in the period can be related to the chirped bandwidth, $\Delta\lambda_{\text{chirp}}$ of the fiber grating as

$$\begin{aligned}\Delta\lambda_{chirp} &= 2n_{eff}(\Lambda_{long} - \Lambda_{short}) \\ &= 2n_{eff}\Delta\Lambda_{chirp}\end{aligned} \tag{7.1.1}$$

The reflection from a chirped grating is a function of wavelength, and therefore, light entering into a positively chirped grating (increasing period from input end) suffers a delay τ on reflection that is approximately

$$\tau(\lambda) \approx \frac{(\lambda_0 - \lambda)}{\Delta\lambda_{chirp}} \frac{2L_g}{v_g}, \qquad \text{for } 2n_{eff}\Lambda_{short} < \lambda < 2n_{eff}\Lambda_{long}, \tag{7.1.2}$$

where λ_0 is the Bragg wavelength at the center of the chirped bandwidth of the grating, and v_g is the average group velocity of light in the fiber.

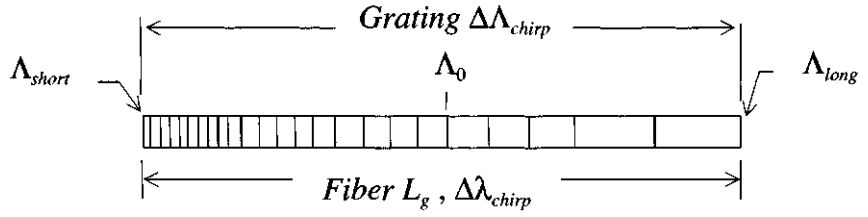

Figure 7.1: The chirped grating.

The effect of the chirped grating is that it disperses light by introducing a maximum delay of $2L_g/v_g$ between the shortest and longest reflected wavelengths. This dispersion is of importance since it can be used to compensate for chromatic dispersion induced broadening in optical fiber transmission systems. At 1550 nm, the group delay τ in reflection is ~10 nsec/m. Therefore, a meter-long grating with a bandwidth of 1 nm will have a dispersion of 10 nsec/nm.

An important feature of a dispersion-compensating device is the figure of merit. There are several parameters that affect the performance of chirped fiber Bragg gratings for dispersion compensation. These are the insertion loss (due to <100% reflectivity), dispersion, bandwidth, polarization mode-dispersion, and deviations from linearity of the group delay and group delay ripple. Ignoring the first and the last two parameters for the moment, we consider the performance of a chirped grating with linear delay characteristics, over a bandwidth of $\Delta\lambda_{\text{chirp}}$. Priest and Giallorenzi [35] have proposed a figure of merit for coherent communications, but taking into account only the dispersion and the bandwidth of the filter. This approach, while not entirely appropriate for chirped gratings owing to the larger parameter set, is never the less a guide in assessing the usefulness of the "ideal" chirped grating. It should be remembered that chirped gratings have a limited bandwidth over which the dispersion is useful, making them different from other truly broadband compensating devices, such as dispersion-compensating fiber [36].

We consider the propagation of an optical pulse in normalized units, in a frame of reference moving in the $+z$ direction at a group velocity v_g. The pulse amplitude $A(z, \tau)$, with a normalized amplitude $U(z, \tau)$, following Agrawal [37], is described as

$$A(z,\tau) = \sqrt{P_{in}}U(z,\tau)e^{-\alpha z/2}, \tag{7.1.3}$$

in which α is the attenuation coefficient of the fiber, P_{in} is the input power, and the frame of reference normalized to the initial pulse width T_0 is

$$\tau = \frac{1}{T_0}\left(t - \frac{v_g}{z}\right). \tag{7.1.4}$$

For a Gaussian pulse with a $1/e$- intensity half-width of T_0, the normalized amplitude is [38]

$$U(0,T) = e^{-T^2/2T_0^2}. \tag{7.1.5}$$

Transmission in a linearly dispersive system broadens the pulse, but does not change its shape, and is simply related to the input pulse width by [37]

$$\left(\frac{T_1}{T_0}\right)^2 = 1 + \frac{z}{L_D}, \tag{7.1.6}$$

which is the well-known formula for linear pulse broadening, remembering that the dispersion length is a function of the spectral width of the pulse and the linear group velocity dispersion (GVD) of the fiber, β_2, as

$$L_D = \frac{T_0^2}{\beta_2}. \tag{7.1.7}$$

Combining Eqs. (7.1.6) and (7.1.7) leads to

$$\left(\frac{T_1}{T_0}\right)^2 = 1 + \frac{z\beta_2}{T_0^2}. \tag{7.1.8}$$

Since the effect of dispersion in a linear system is additive, we may now modify the GVD parameter β_2 by including the dispersion of the grating for the bandwidth of the pulse so that the pulse broadening is

$$\left(\frac{T_1}{T_0}\right)^2 = 1 + \frac{\beta_2}{T_0^2} z + \frac{\beta_g}{T_0^2} L_g, \tag{7.1.9}$$

where β_g is the GVD of the grating of length L_g. We note that the dispersion D_f of the fiber is related to the GVD by [37]

$$\beta_2 = \frac{\lambda^2}{2\pi c} D_f. \tag{7.1.10}$$

A similar expression relates the fiber grating dispersion D_g to the grating GVD, but with the sign depending on the sign of the grating chirp. We now find that the pulse broadening for the Gaussian pulse is

$$\left(\frac{T_1}{T_0}\right)^2 = 1 + 2\pi c \frac{\Delta\lambda^2}{\lambda^2} (D_f z + D_g L_g), \qquad \text{for } \Delta\lambda \leq \Delta\lambda_{chirp}. \tag{7.1.11}$$

In Eq. (7.1.11) we have used the relationship between a transform-limited pulse width and its spectrum ($\delta\omega T_0 = 1$).

Note the stipulation on the bandwidth of the pulse, since dispersion compensation is only valid for the bandwidth of the grating. If the pulse bandwidth is larger, then the pulse recovery is

$$\left(\frac{T_1}{T_0}\right)^2 = 1 + \frac{2\pi c}{\lambda^2}(\Delta\lambda^2 D_f z + \Delta\lambda_{chirp}^2 D_g L_g), \qquad \text{for } \Delta\lambda > \Delta\lambda_{chirp}. \tag{7.1.12}$$

For perfect recompression, $D_f z = -D_g L_g$, and the pulse remains unaltered at the output of the fiber, so long as the bandwidth of the pulse is smaller than the bandwidth of the grating. We can now define a figure of merit (FOM) for the bandwidth of the grating, since the maximum compression ratio that can be achieved is

$$\left(\frac{T_1}{T_0}\right)^2 = 1 + \frac{2\pi c}{\lambda^2}(\Delta\lambda_{chirp}^2 D_g L_g) = 1 + M^2. \tag{7.1.13}$$

We can redefine Eq. (7.1.13) by recognizing that the dispersion D_g of the grating is almost exactly 10 nsec/m/$\Delta\lambda_{\text{chirp}}$, so that

$$M^2 = \frac{2\pi c}{\lambda^2}(\Delta\lambda_{chirp} L_g \times 10^{-8}). \tag{7.1.14}$$

We note that the FOM is proportional to the square root of the length and the chirped bandwidth of the grating. Here, we remind ourselves that we have used the 1/*e* bandwidth of the grating. The conversion from the Gaussian 1/*e* width to its FWHM width, which is more commonly used, may be done by using the following relationship:

$$\frac{T_{FWHM}^2}{T_0^2} = 4 \ln 2. \tag{7.1.15}$$

It is clear from Eq. (7.1.13) that the pulse broadening, which can be compensated for, is

$$\Delta T^2 = T_1^2 - T_0^2 = M^2. \tag{7.1.16}$$

As an example, a 1-meter-long grating with a bandwidth of 10 nm will have $M = 280$. This means that an input pulse can undergo a pulse broadening of ~280 times its initial pulse width and be recompressed. The dependence of the FOM on the grating bandwidth for maximum

recompression is shown in Fig. 7.2. In the simple analysis just given, it is necessary to recognize that the chirped grating response is far from ideal. The actual reflection and detailed delay characteristics can have a profound influence on the performance, especially when the grating is to be used for compensation of large dispersion in ultrahigh-bit-rate systems. However, the FOM is a good indicator of the best possible performance of a grating and may be used to compare the performance achieved with gratings. Ultimately, the most important parameters that characterize a transmission link's performance are the bit-error rate (BER), loss penalty, and error floor. The influence of deviations from ideal transfer characteristics on the BER and loss penalty is considered in Section 7.5.

7.2 Chirped and step-chirped gratings

We have seen the theory of fiber Bragg gratings in Chapter 4. Although it is possible to mathematically express the coupled modes in a way that exactly mimics the grating function, the methods of computation are numerical, since no suitable analytical solutions are available. The transfer matrix method (TMM) is ideally suited to chirped gratings, since the grating may be broken up into smaller sections of uniform period and/or refractive index profile. While there are other methods for extracting the

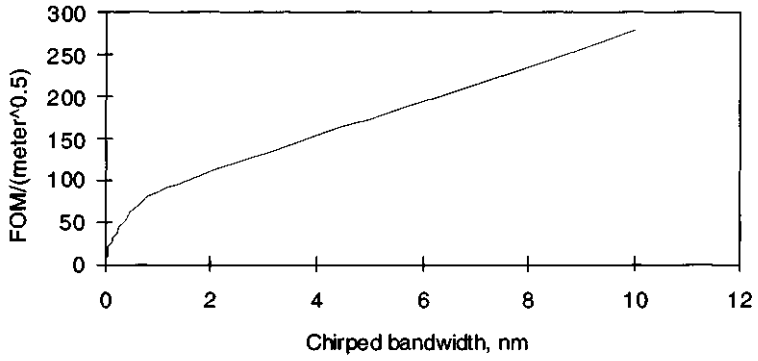

Figure 7.2: The maximum pulse re-compression FOM per $\sqrt{}$(meter) of grating length. For optimum compression, the bandwidth of the pulse is the same as the chirped grating bandwidth. As the bandwidth gets smaller, the pulse width becomes larger, so that the figure of merit drops.

reflection, transmission, and group-delay response (see Chapter 4), in the following we use the TMM approach to evaluate the transfer characteristics of arbitrarily chirped gratings. There are naturally limitations to the application of the TMM. Since coupled mode analysis depends on the slow variation of the parameters of the grating as a function of the wavelength of light, e.g., chirp, refractive index modulation, and coupling constant κ_{ac}, it is not possible to compute entirely "arbitrary" gratings (see Chapter 4, Grating Simulation). Apart from this limitation, there are other questions that need addressing: for example, in the synthesis of chirped fiber Bragg gratings, what constitutes a continuous chirp in view of the fact that most gratings exhibit quasi-continuous chirp, and the influence of apodization on the dispersion and reflection characteristics. First it is necessary to view the grating as a physical entity, in which coupling parameters are a weak function of space. Thus, it may be seen that a chirped grating, shown in Fig. 7.3, is merely a uniform period grating that has been slightly perturbed.

How many sections do there need to be in grating (c) for it to be indistinguishable from a grating that is continuously chirped (b)? In other words, how small can the chirp parameter, $d\phi(z)/dz$ [Eqs. (4.3.9) and (4.3.10)] be for a given length of grating? In order to answers this question, we consider the bandwidth characteristics of the uniform period Bragg grating. We note that the bandwidth of an unchirped grating section δl is

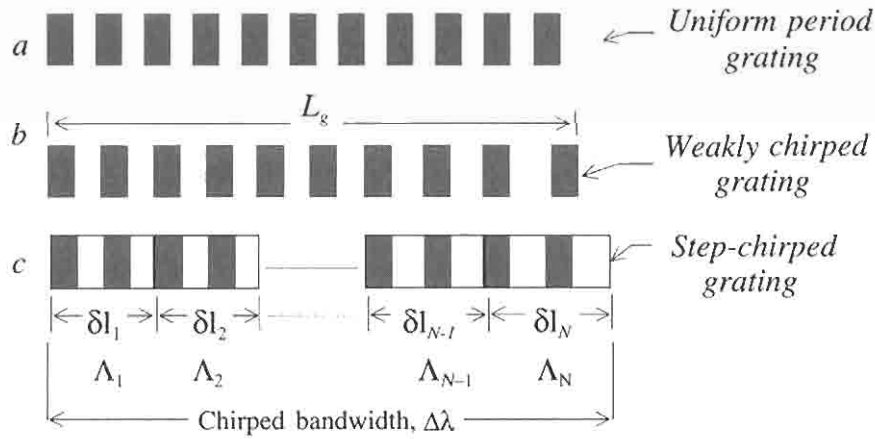

Figure 7.3: A uniform grating (a), a weakly chirped grating (b), and a step chirped grating (c).

$$\delta\lambda = \frac{\lambda^2}{2\pi n_{eff}\,\delta l}\sqrt{(\kappa_{ac}\delta l)^2 + \pi^2}, \tag{7.2.1}$$

from Eq. (4.6.14), and we have assumed that each section is identical in length δl. For most of the gratings of interest here, we assume that $(\kappa\delta l)^2 \ll \pi^2$. The phase matching condition for the section requires that

$$\lambda_{Bragg} = 2\Lambda_g n_{eff}, \tag{7.2.2}$$

where Λ_g is the period of the grating section. The period is nearly constant for gratings with a small percentage chirp. Remembering that $\delta l = L_g/N$, we get

$$\frac{N}{L_g} = \frac{2n_{eff}\,\delta\lambda}{\pi\lambda_{Bragg}^2}. \tag{7.2.3}$$

When $N = 1$, the bandwidth of the grating is simply the bandwidth $\Delta\lambda'$ of the unchirped grating of length L_g. For the chirped grating with a bandwidth $>\Delta\lambda'$, made of sections, the bandwidth of each section can only be greater than the bandwidth of the unchirped grating (being shorter in length), but can equal the bandwidth of the chirped grating only if it is the appropriate length. Applying the relationship [Eq. (7.2.3)] for bandwidths greater than the unchirped bandwidth, $\Delta\lambda'$, we simply allow the bandwidth of each section to be identical to the bandwidth $\Delta\lambda_{chirp}$ of the chirped grating, i.e.,

$$\delta\lambda = \Delta\lambda_{chirp}, \tag{7.2.4}$$

so that for a fiber Bragg grating at a wavelength of 1550 nm, $N/L_g \cong 0.4\Delta\lambda_{chirp}$ steps/(mm-nm). Finally, we arrive at the relationship between the number of steps per unit length and the chirped bandwidth,

$$\frac{N}{L} = \frac{2n_{eff}\,\Delta\lambda_{chirp}}{\pi\lambda_{Bragg}^2}. \tag{7.2.5}$$

Here λ_{Bragg} is the central Bragg wavelength of the chirped grating. The simple relationships of Eqs. (7.2.4) and (7.2.5) are minimum requirements for the step chirped grating and should approximate to a continuously chirped grating. It may be seen immediately that there is an intuitive feel about the conclusion — that the bandwidth of each step of the grating should be at least as large as the chirp of the whole grating. Increasing the number of steps, i.e., $\delta l \to 0$, approaches the continuously chirped

grating. A more detailed analysis [39] bears out the simple conclusion; a more accurate (to 1%) fit increases the bandwidth of each step by only 40% [39]. Curiously, the comparison between gratings of the same chirp but different number of steps gets better if the total chirp is reduced by $\Delta\lambda_{chirp}/N$. The convergence to the asymptotic transfer characteristics is faster for all SCGs with the chirp bandwidth adjustment, although this is especially true for those with a few sections. For a large number of sections, this really does not matter. For all the following simulations, the bandwidth adjustment has been included.

Figures 7.4 and 7.5 show the calculated reflectivity and delay, respectively, of an SCG (L_g = 100 mm, $\Delta\lambda_{chirp}$ = 0.75 nm) grating with 200 sections (2 steps/mm) and an SCG with only 0.42 steps/mm [total steps = 42, according to Eq. (7.2.5)]. It is immediately apparent that the agreement between the two spectra is good. The reflectivity spectrum has a ripple that is characteristic of unapodized gratings, as does the group delay. The strong ripple in the group delay plays an important role in the recompression of a dispersed pulse. While there is an average delay slope, the ripple frequency becomes smaller toward the end from which the reflection is measured. This is true for even continuously chirped gratings, and the influence of apodization is examined in Section 7.3.

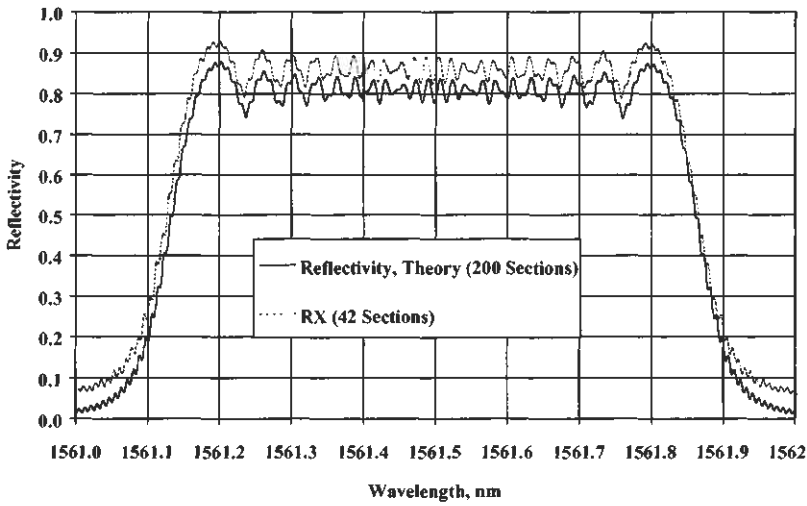

Figure 7.4: Reflectivity of a 100-mm-long SCG with 200 sections as well as 42 sections. The reflectivity curves have been offset to allow easy examination.

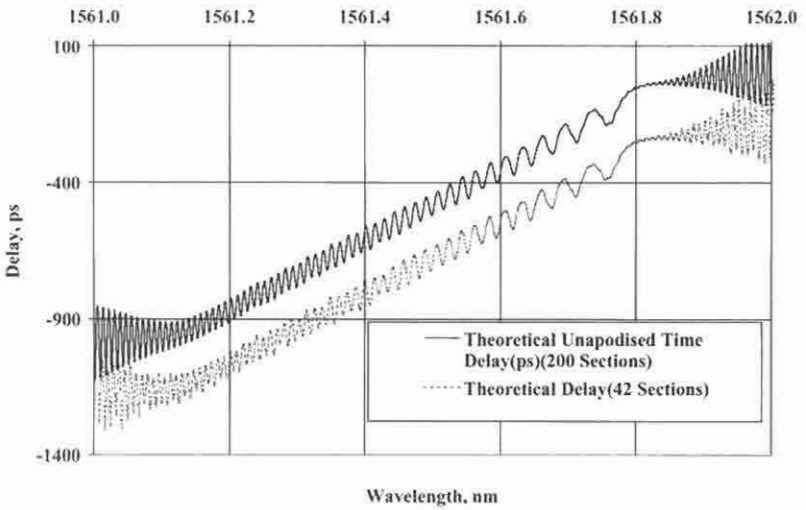

Figure 7.5: Comparison of the delay characteristics of the SCGs shown in Fig. 7.4. For the 200-section grating, $N/L_g = 2$ steps/mm, while for the 42-section grating, $N/L_g = 0.42$ steps/mm.

We now examine a 4-mm-long SCG with a chirp of 1 nm. The minimum number of sections of this grating according to Equation (7.2.5) is 2. Simulations of the reflectivity and delay are shown in Figs. 7.6 and 7.7, respectively, for two and three sections. Along with these gratings the characteristics of a 50-section grating is also shown. The grating characteristics are surprisingly similar despite the few sections, especially noting the positions of the zeroes and the central part of the reflection spectrum. The agreement is equally valid for apodized fiber Bragg gratings [39]. For convenience, it may be simple to double the minimum number of calculated sections for good linearly chirped gratings.

The design of quasi-linearly chirped gratings has been represented graphically in Fig. 7.8. This design diagram shows that a grating must be divided into a minimum number of sections per millimeter for a given chirp, irrespective of the length of the grating. The criterion used for the design is that the total group delay of a continuously chirped grating with the same coupling constant and length as the step-chirped grating should differ by less than 1% of its maximum value. For example, the maximum deviation in the delay ripple in a 100-mm-long unapodized grating should be less than 10/psec across 90% of the available bandwidth. This result

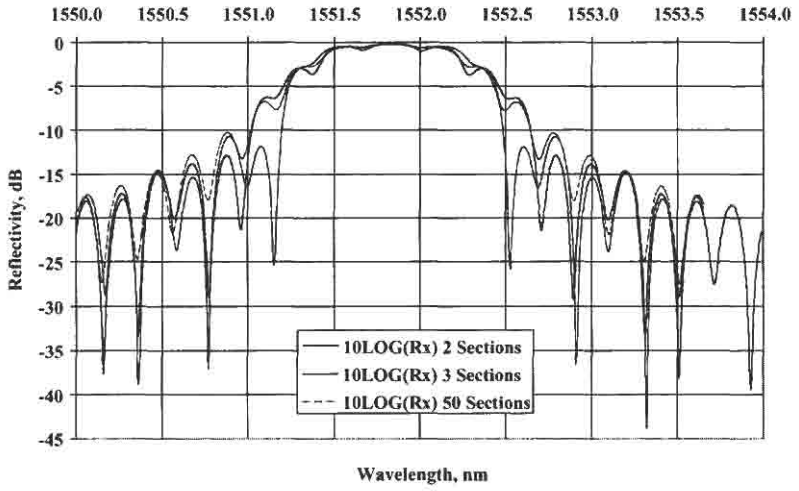

Figure 7.6: The reflectivity of 4-mm-long, 1-nm chirp SC gratings with 50 (dashed line: N/L_g = 12.5 steps/mm), 2 (gray line: N/L_g = 0.5 steps/mm), or 3 sections (continuous line: N/L_g = 0.75 steps/mm).

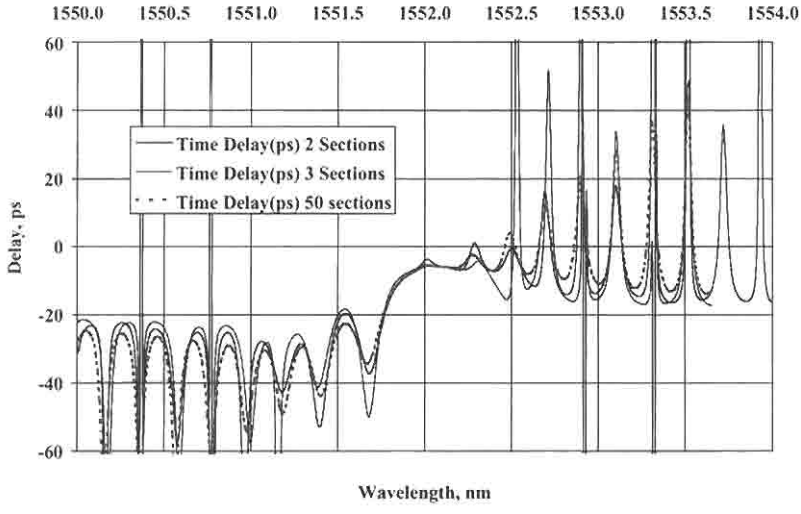

Figure 7.7: Theoretical delay of 4-mm-long, 1-nm chirp SC gratings with 50 (dashed line), 2 (grey line), and 3 (continuous line) sections. Notice that even with so few sections as determined by the simple relationship of Equation (7.2.5), the characteristics are very similar.

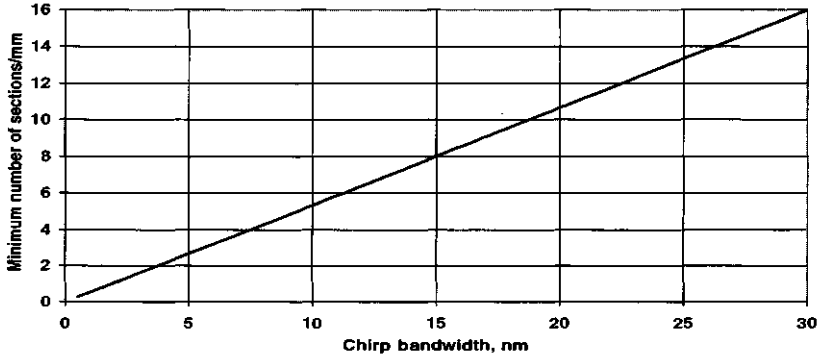

Figure 7.8: Design diagram for step-chirped gratings (Reprinted from Kashyap R., "Design of step chirped gratings," *Optics Commun.*, Copyright (1997), 461–469, with permission from Elsevier Science. Ref [39]).

is numerically evaluated and serves as a useful guide for a variety of chirped gratings [39].

We now consider the effect of having far fewer sections than the required minimum in a chirped grating. When this happens, the bandwidth of each section is no longer sufficient to overlap with the bandwidth of succeeding sections, so that the reflection spectra break up into several discrete peaks, each representing the effect of the single sections. However, the residual reflections due to the edges of the gratings (start/stop, see Section 7.4) do interfere with the others, causing the peaks to be altered from the smooth curves of uniform period gratings. The transmission spectrum of a 5-nm bandwidth, 8-mm-long grating is shown in Fig. 7.9 for two values of refractive index modulation: A, Δn = 4e-4 and B, Δn = 1e-3, as well as a continuously chirped grating (C, Δn = 1e-3). Note that while the increase in the reflectivity smoothes out the structure, the spectrum deviates from the continuously chirped grating spectrum. In particular, the side-lobe structure, which is absent in curve C, is obviously present in curve B.

For the design of broadband reflectors, it is important to incorporate the correct number of sections; otherwise, the dispersion characteristics will suffer dramatically, as will the out-of-band reflectivity. The out-of-band reflection in continuously chirped gratings is generally apodized, since the distributed reflections from all the "different" sections may be thought to add in a way that averages out any coherent buildup. Within

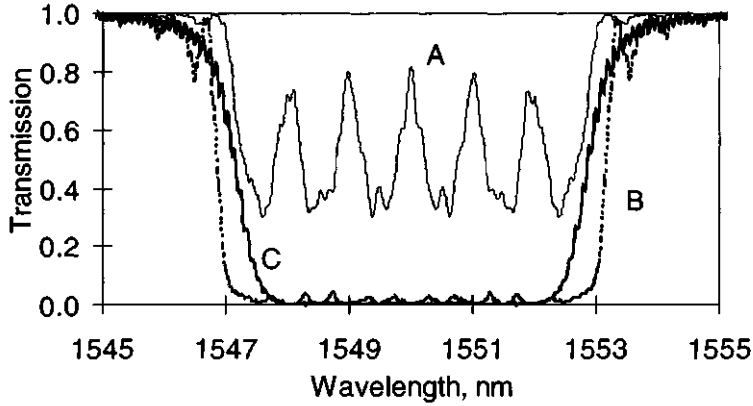

Figure 7.9: The effect of too few sections in a grating of length 8 mm with a bandwidth of 5 nm. For 6 sections and a small refractive index (A, 0.75 sections/mm, $\Delta n = 4 \times 10^{-4}$) the spectrum breaks up into individual peaks. The minimum number of sections for a continuously chirped grating is 3 sections/mm. For stronger refractive index modulation (B, $\Delta n = 1 \times 10^{-3}$), the grating "appears" continuously chirped. However, neither the delay (not shown) nor the reflectivity spectrum matches those of the continuously chirped gratings, C.

the band, it is an entirely different story. The edges of a grating have a large impact on the reflection ripple as well as the delay ripple, as seen in Figs. 7.4 and 7.5. Consequently even small broadband reflections can change the ripple in the delay spectrum.

7.2.1 Effect of apodization

In Chapter 5 we saw the effect of apodization on gratings; the immediate effect was the dramatic reduction in the side-lobe levels in the reflection spectrum. Chirped gratings tend to have lower side-mode structure in their reflection spectra to begin with, and the advantage of apodization is in the reduction of internal interference effects that cause the group delay to acquire a ripple. We consider here the properties of chirped gratings, which have reflectivities of the order of 10 dB, suited to the compensation of linear dispersion in fibers, and study the influence of apodization. While the details of both the reflection and group delay spectra change with the strength of the coupling constant of the grating, general observations remain essentially unchanged. The chirped grating

is a continuously distributed reflector. Ideally, light entering into a chirped grating from one end should be dispersed in exactly the opposite way when entering from the other end. Early measurements on chirped gratings did show this feature [40]. However, the gratings were short, had a large bandwidth, and consequently had a small dispersion. Dispersion is not generally reversible with unapodized chirped gratings. To understand this phenomenon, we remind ourselves that light entering from the short-wavelength end of a highly reflective chirped grating is reflected such that only a small fraction of the short-wavelength light penetrates through to the other end of the grating, while the long-wavelength light does. On entering from the long-wavelength end of the grating, exactly the opposite occurs. The detailed delay ripple is a result of the interference between the broadband reflection due to the edge of the grating and the distributed nature of the reflection of the grating [41].

As a crude comparison, when light enters from the long-wavelength end of the grating, the interference is predominantly due to the large long-wavelength reflection from the front of the grating and the small broadband reflection due to the front edge. Short-wavelength light penetrates the dispersive grating and is predominantly reflected from the rear end; it, too, interferes with the low broadband reflection from the front end. In neither case does the rear end of the grating play a strong role. Since the dispersion increases with greater penetration into the grating, the delay ripple frequency increases with decreasing wavelength (see Fig. 7.5). With the launch direction reversed, exactly the opposite occurs: The delay ripples increase in frequency with increasing wavelength. Therefore, light dispersed by reflection from the short-wavelength end of the chirped grating *cannot be undone* by reflection from the long-wavelength end! The simulated result of this asymmetry is shown in Fig. 7.10. The sign of the frequency chirp in the delay ripple is insensitive to the launch direction i.e., the frequency of the chirp is always from a low to a high frequency (Fig. 7.10, B and C) when viewed from either end.

The role played by the rear end of the grating is apparent when the coupling constant κ_{ac} is apodized asymmetrically. In this example we consider a grating with a profile of the refractive index modulation as shown in Fig. 7.11a. The grating profile is half-cosine apodized so that the light launched from the long-wavelength end sees a gradually increasing coupling constant. The amplitude of the light reflected from the front end of the grating is now lower than in an unapodized grating, and long-wavelength light penetrates more deeply so that the amplitude at the

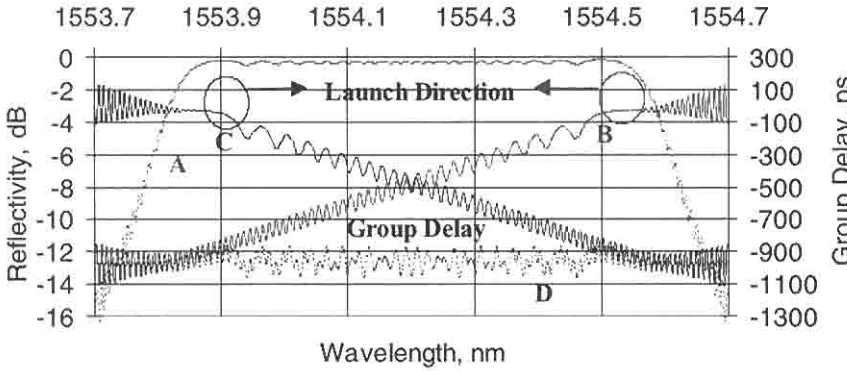

Figure 7.10: Reflection and delay spectrum of an unapodized 100-mm-long grating with a chirped bandwidth of 0.75 nm. The reflection spectrum remains unchanged when measured from either end (A). The group delays (B and C) have been computed for light launched in the direction shown, from the short-wavelength end (B) and the long-wavelength end (C). The net dispersion, which is the sum of the two, is shown as curve D. This residual dispersion prevents full recompression of a pulse dispersed by the grating.

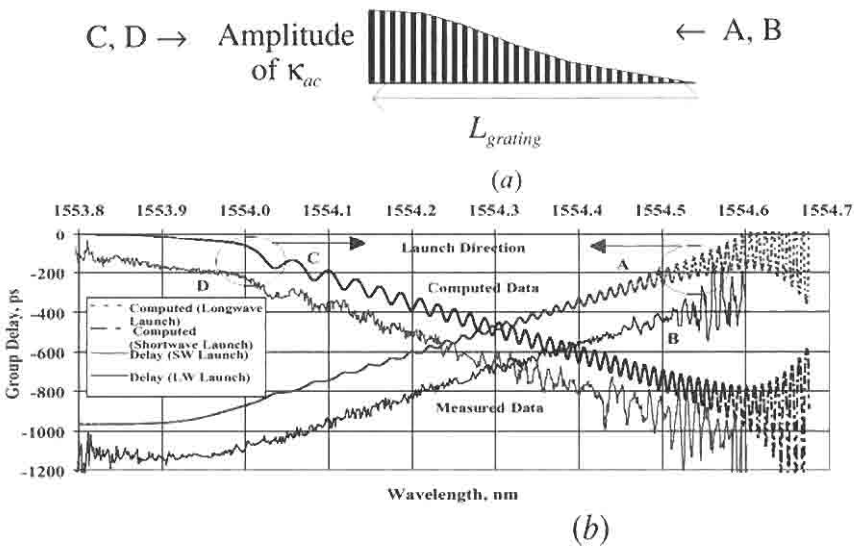

Figure 7.11: Apodization profile of the half-cosine long wavelength-edge apodized chirped grating is shown on above the figure in (a). Measured and computed group delay (b), when measured in both directions.

rear end is higher than in the unapodized grating. The broadband reflection from the input of the grating has now been reduced significantly due to apodization. Hence, the ripple should disappear on the long-wavelength end. However, we notice that the ripple is of the order of that of the unapodized grating, but now *of higher frequency* at the input end, Fig. 7.11b, A. This is indicative of interference from the reflection off the rear end of the grating. Note, too, that the ripple has the *lowest frequency* and disappears at the shortest wavelengths, quite the reverse of the unapodized grating, with reduced interference from the launch end (due to apodization). The corresponding measured result for this type of a grating is shown in Fig. 7.11b, B [42].

On the other hand, when light is launched into the short-wavelength end, the reflected delay ripple is almost *identical* to that of an unapodized grating (Fig. 7.11b, C and D). The apodized long-wavelength end does not play a role in generating the delay ripple.

This result is of particular importance for long chirped gratings. When one half of a grating remains unapodized while the other half is cosine apodized, the results are even more dramatic, as shown in Fig. 7.12. Shown in curve A is the group delay of an unapodized grating, while B and C refer to the grating profiles shown above the figure in (B) and (C) with light launched in the directions shown for each grating. The group delay ripple measured from the long wavelength end, B, has all but disappeared for the long-wavelength apodized grating, and the residual ripple at the long-wavelength edge is again due to the interference from the short-wavelength end. For light launched into the long-wavelength end in the short-wavelength apodized grating (C), the group delay ripple C is as for the unapodized grating, A.

The implication of the apodization is as follows: Long chirped gratings for dispersion compensation require apodization only on the long wavelength end of the grating. The type of apodization (see Chapter 5) will determine the bandwidth reduction in the reflectivity spectrum. The unapodized short wavelength end, provides extra bandwidth, with a small penalty on the long wavelength end due to the residual ripple.

An important factor, that influences the performance of chirped gratings in dispersion compensation is the deviation of the delay from linearity and group delay ripple. Symmetrically apodized gratings offer the prospect of excellent dispersion compensation [43]. The group delay differences from linear delay and reflectivity for commonly found cosine and raised cosine profile apodized gratings are shown in Fig. 7.13. The gratings have

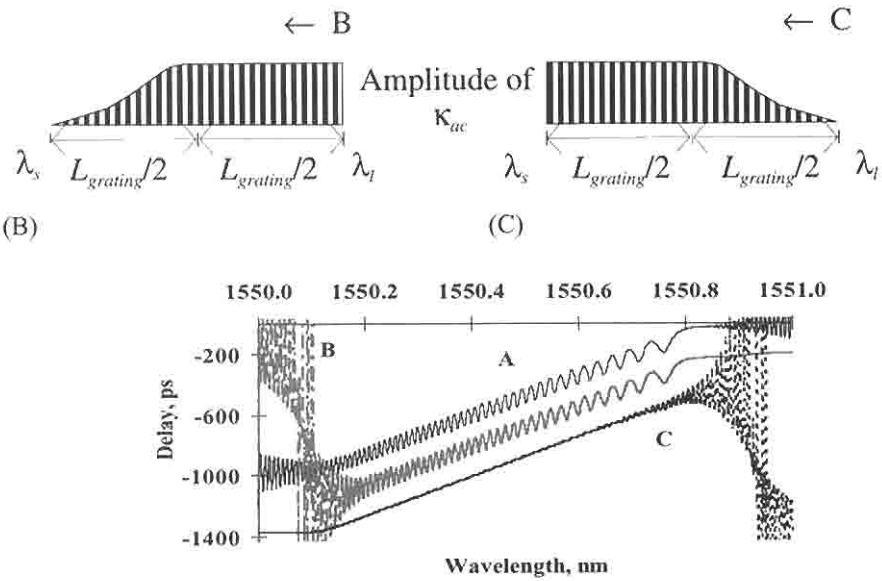

Figure 7.12: Apodization profiles (half-cosine over half the grating) and respective launch directions shown in (B) and (C). Group delay compared for long wavelength launch into a grating, A: unapodized, B: short-wavelength apodized, and C: long-wavelength apodized (after Ref. [42]).

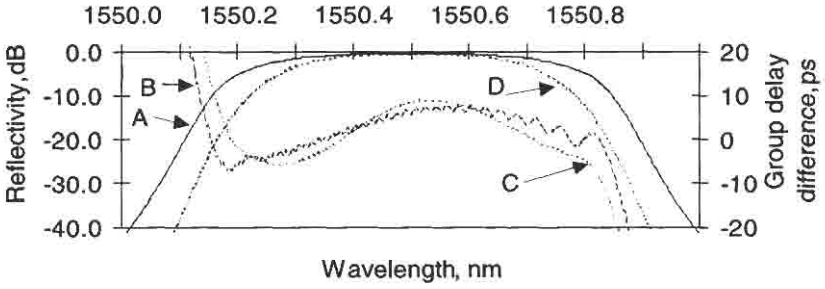

Figure 7.13: Reflectivity (A) and group delay difference (B) of cosine apodized grating as well as reflectivity (D) and group delay difference (C) for raised cosine apodized grating.

a peak reflectivity of ~90% and are 100 mm long with a bandwidth of 0.75 nm (D_g = ~1310 psec/nm), designed for compensation of the dispersion of 80 km of standard telecommunications fiber (D_f = 17 psec/nm/km). The group delays have two features in common: The dispersion curves deviate from linearity slowly across the bandwidth of the grating, and they are flat within ±5 psec. With higher-reflectivity gratings, the curvature worsens. Note, however, that the stronger, raised cosine apodization eliminates the delay ripple almost entirely, but reduces the available bandwidth. Roman and Winnick [44] have shown that using Gel'fand–Levitan–Marchenko inverse scattering analysis, it is possible to design a grating with a near perfect amplitude and quadratic phase response to recompress transform limited pulses.

With asymmetric apodization as shown in Figs. 7.11 and 7.12, apodizing only one end of the grating has a beneficial effect of better bandwidth utilization than symmetrically apodized gratings, since less of the grating length is used in the apodization process. There is a slight increase in the peak-to-peak group delay ripple on the long-wavelength side, as seen in Fig. 7.12, but it is still <5 psec over a wider bandwidth. With a stronger coupling constant and a different apodization function (e.g., tanh), we note that less of the light reaches the rear end of the grating, so that the ripple reduces still further. However, the curvature also increases. Figure 7.14 shows the reflection and group delay difference spectra of a symmetric

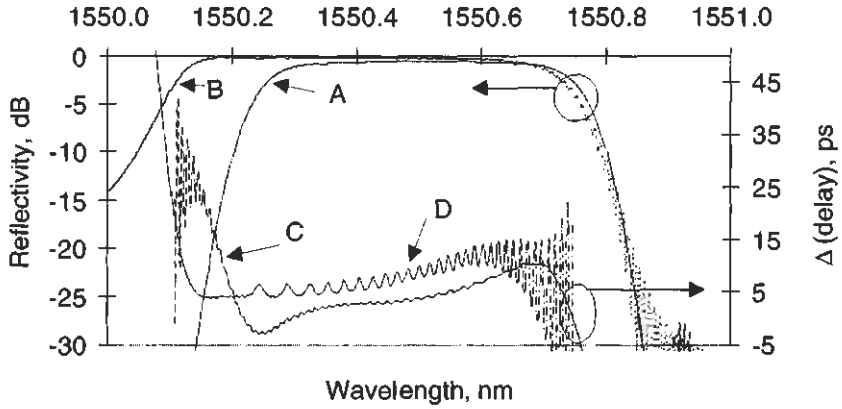

Figure 7.14: Comparison between the delay and reflection spectra of asymmetrically (B, D), and symmetrically (A, B) apodized gratings.

and an asymmetric tanh apodized grating. The bandwidth of the asymmetric apodized grating, B, is now wider than that of the symmetric apodised grating, A, and so is the group delay difference, D. The peak reflectivity of B is 98%, whereas that of A is 90%. There is also a small ripple acquired in both the reflection and group-delay spectra (C and D). With lower reflectivity, the ripple in the asymmetrically apodized grating *increases,* rather than decreasing as is the case with the symmetrically apodized grating [41].

7.2.2 Effect of nonuniform refractive index modulation on grating period

During fabrication, it is necessary to ensure that the grating receives the correct UV dose along its length. If the dose varies, so does the effective refractive index modulation and therefore κ_{ac}. A constant increase in the UV dose with length merely chirps the grating. However, *random* variations are generally common with pulsed lasers, since the UV radiation has hot spots across the beam, with the result that the grating is no longer uniformly exposed. While this may not be a problem for many filtering applications, it does degrade the performance of the group delay in chirped gratings, limiting performance. Ouellette [4] reported the effect of a noisy refractive index profile and dither in the period of the grating on the reflection and dispersion characteristics. It was found that, apart from a general increase in the out-of-band reflection, the group delay was also degraded. A period variation of 0.03 nm (~5%) over a length scale of 1 mm degraded the delay spectrum substantially. This is a serious issue for the fabrication of high-quality gratings. Even with perfect phase masks, such factors as the random variations in the effective index of the mode, UV dose, or vibration during fabrication will cause deterioration in the quality of the grating.

We consider the likely effect of a maximum variation of ~10% of the refractive index modulation amplitude, Δn (7.5×10^{-5}), but over different scale lengths of 50, 100, and 200 microns. These are expected to be typical regions over which the refractive index modulation varies. In order to model this behavior, we have assumed that each section of the scale length varies in the index modulation entirely at random with a *maximum* value of 1×10^{-5}. This is realistic despite the averaging effect of multiple pulse exposure, since the peak UV intensities can fluctuate over several orders. The results of the simulations of the deviation from linearity of the delay

and the transmission spectra are shown in Figs. 7.15 and 7.16. The uniformly exposed curve A is degraded rapidly on the 50 micron length scale with a high frequency ripple (C), to a slowly varying, more uniform, but larger-amplitude ripple across the spectrum with increasing length scale (C to D). The last curve D is consistent with observations of delay ripple variation [45].

It is very difficult to distinguish small differences from the reflection spectra of high reflectivity gratings [4]. We therefore choose to observe the grating transmission spectra, which can clearly resolve these differences. Figure 7.16 shows the transmission spectra, shifted vertically in order to highlight the small changes in the curves, using the same data as in Fig. 7.15. The noise on the spectra is apparent, although the energy in the reflected light is only slightly affected. The significant effect of the noisy profile is on the delay ripple. The variation $\delta\lambda_{Bragg}$ in the Bragg wavelength as a function of the change in the refractive index $\Delta\delta n$ and the grating period $\delta\Lambda_g$ is

$$\delta\lambda_{Bragg} = 2\Lambda_g \eta \delta\Delta n + 2n_{eff}\,\delta\Lambda_g, \tag{7.2.6}$$

where η is a core overlap factor of ~0.9. The shift in the Bragg wavelength

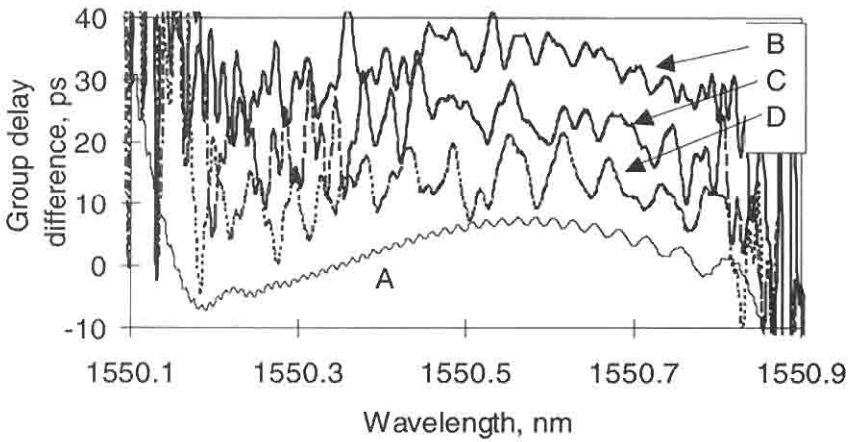

Figure 7.15: Group delay difference from a slope of 1310 psec/nm for cosine apodized 100-mm-long grating (90% reflector) with no variation (A) in the refractive index modulation, $\delta\Delta n$; random variation of up to 1×10^{-5} over a length scale of 50-micron sections (B); 100-micron sections (C); and 200-micron sections (D).

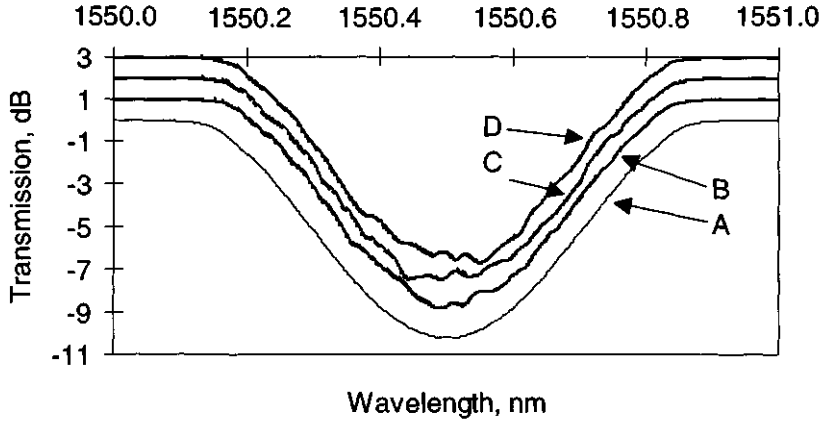

Figure 7.16: The transmission spectra of four cosine apodized gratings (L_g = 100 mm, $\Delta n = 7.5 \times 10^{-5}$, $\Delta\lambda_{chirp}$ = 0.75 nm) as a function of random variation in the refractive index modulation. A has $\delta\Delta n = 0$; B, C and D have a maximum random variation $\delta\Delta n = 1e \times 10^{-5}$ over length scales of 50, 100, and 200 microns, respectively, as in Fig. 7.15.

amounts to ~10 pm at a wavelength of 1550 nm for an index change of 1×10^{-5}. The same change in the wavelength occurs for a random variation in the Bragg wavelength period $\delta\Lambda_g$ of ~3.42pm.

7.3 Super-step-chirped gratings

Chapter 3 introduces the fabrication of ultralong gratings. One of the methods of generating ultralong gratings is by stitching together a set of short chirped gratings, to form the super-step-chirped grating (SSCG) [46]. The structure is schematically shown in Fig. 5.18, Chapter 5. Here we consider the influence of an imperfect stitch between two sections of the SSCG. Figure 7.17 shows three step-chirped gratings with gaps in between. The first SCG (LHS) begins at λ_1 and finishes at λ_2, in N sections, each with an integral number of periods. The number of periods is adjusted so that each section is nominally the same length within the length of a period. The second SCG begins with a period $\lambda_2 + \delta\lambda$ and ends at a period $\lambda_2 + (N - 1)\ \delta\lambda$. The two gratings are written sequentially, ideally with zero gap in between. In a perfect grating, the periods would simply follow

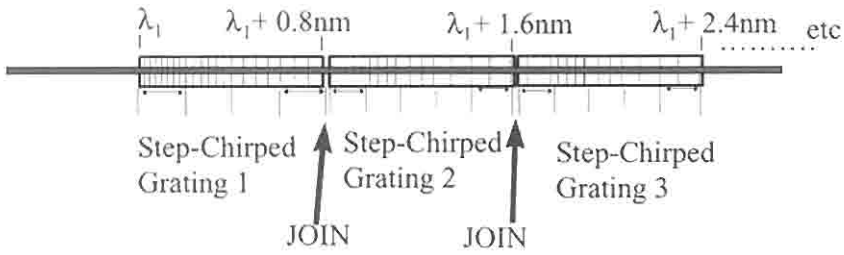

Figure 7.17: A schematic of the super-step-chirped grating (SSCG). Each grating is of nominally an identical integer number of periods [47].

each other, without a perturbation. In reality, unless care is taken, there is a small error $\delta l/\Lambda_2$ at the join. This error will ultimately have an effect on the performance of the grating.

We now compare this with a uniform period grating with a phase step. A phase step of a quarter wavelength, as we have seen in Chapter 6, introduces a bandgap in the reflection spectrum. The effect is similar in gratings, which have a small chirp, since the Bragg wavelengths of two adjacent sections are only slightly different, and the reflection spectrum is strongly overlapped. This is indeed the case with SCGs and is shown in Fig. 7.18. The reflection spectrum centered at the wavelength of the join shows the quarter wavelength dependence of the bandgap. However, the dependence changes with increasing gap, but the join is also invisible at

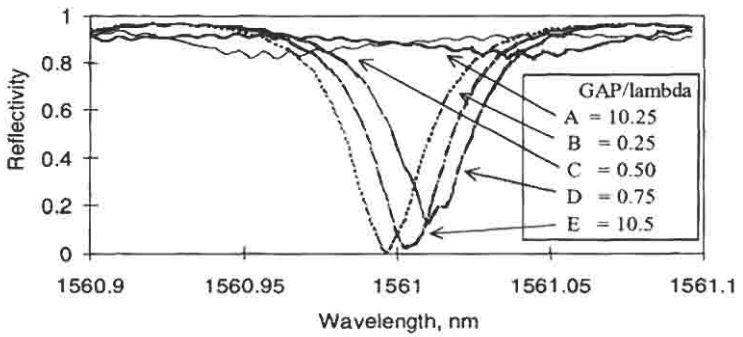

Figure 7.18: The reflection spectrum of the join region of 2 × 100 mm long SCGs as a function of the gap at the join in fractions of the Bragg wavelength. The gratings are 100 mm long with a chirped bandwidth of 0.75 nm each.

a gap of 10.25 λ_{Bragg}. The group delay is more sensitive but is only affected when light crosses the gap. This means that light launched from the long-wavelength end experiences a change in the group delay ripple on the short-wavelength side of the gap, and vice versa when traveling from the short-wavelength end. This has implications for SSCGs made with more than two SCGs. The grating nearest the launch end remains essentially unaffected, while the group delay ripple of subsequent gratings deteriorates.

Figure 7.19 shows the effect of the join on the group delay. At the join, there is a localized discontinuity, which becomes narrower as the gap gets larger, and almost disappears. Simulations have shown that large gaps (5 mm) tend to smooth out the effect of the join, but the delay through the gap does introduce a step change in the group delay on either side of the join.

We see a relative increase in the noise from the long-wavelength end (launch end). In comparison, a 500-mm-long SSCG grating with random stitching errors at every 100 mm is shown in Fig. 7.20 [46]. Here, the stitching produces small spikes at the join, and also a general increase in the noise at the short-wavelength end. These are believed to be due to

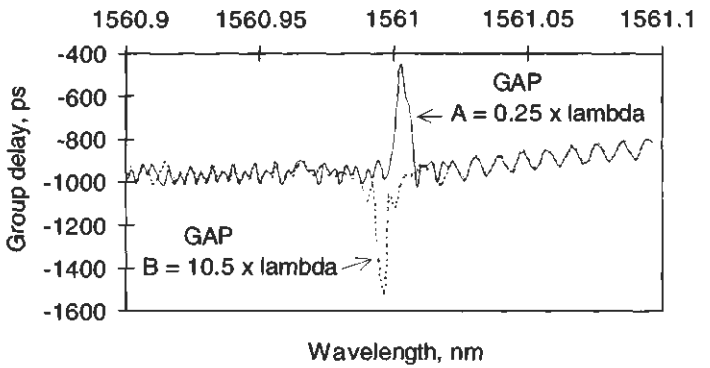

Figure 7.19: The group delay at the join of the gratings shown in Fig. 7.18 for two values of the gap: 0.25 (A) and 10.5 (B) times the Bragg wavelength. The delay spike is localized to the join and is not apparent from the long-wavelength end of the grating. In this simulation, the light enters the long-wavelength end of the grating. The effect is reversed if the light is launched from the short-wavelength end.

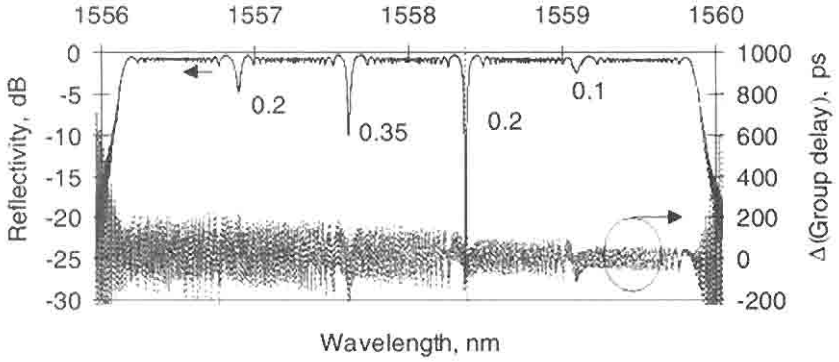

Figure 7.20: The reflectivity and group delay difference of a 500-mm-long SSCG with random stitching errors, shown as a fraction of the Bragg wavelength.

the cumulative effects of each join. However, as has been reported, these gratings may still be useful for dispersion compensation at 10 Gb/sec [48].

In Fig. 7.21 is shown the measured reflectivity and relative group delay characteristics of a 400-mm-long SSCG made in four sections with random stitching errors. We note that the characteristics of the relative group delay are better than the simulation suggests. This is probably due to small random variations in the chirp of each grating section.

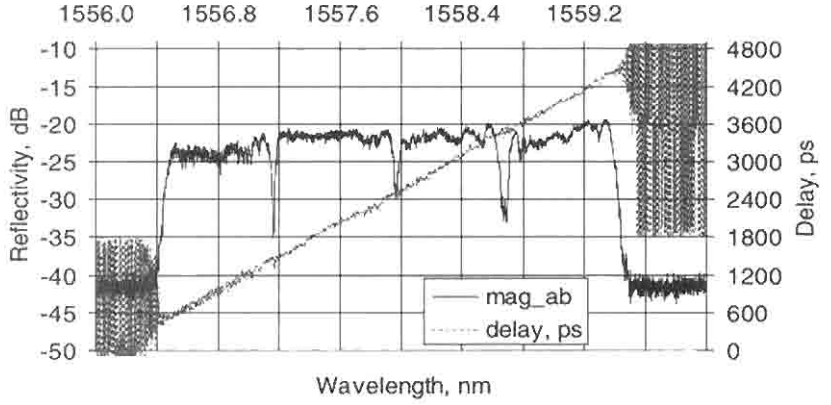

Figure 7.21: The measured characteristics of a 400-mm-long SSCG with a chirped bandwidth of ~3 nm and random stitching errors. Compare with Fig. 7.20.

The computed reflectivity and group delay of a 1.3-meter-long SSCG [48] with a bandwidth of ~10 nm and no stitching errors are shown in Fig. 7.22a. The overall reflectivity is similar to shorter gratings, but as the bandwidth is increased, the shorter wavelength end group delay suffers less from the broadband reflection of the long-wavelength edge of the grating. Note that in this simulation, the resolution of the computation (1 pm) has lost the information on the group delay ripple. Figure 7.22b shows a high-resolution simulation (0.1 pm) of the reflectivity and group delay, to highlight the GDR of the first part of a 1-meter-long unapodized grating. A detail of the group delay ripple of $\sim \pm 60$ ps is shown in Fig. 7.22c.

Long gratings with only a small amount of apodization on the long-wavelength end (normally the input end for dispersion compensation) will remove a substantial part of the group delay ripple and should be useful for transmission rates in excess of 10 Gb/sec.

7.4 Polarization mode dispersion in chirped gratings

An issue that becomes important at high transmission bit rates (>10 Gb/sec) is the effect of polarization mode dispersion (PMD). As the transmission rate increases, the bit period reduces. If any component in the transmission path is birefringent, the different pulse arrival times of the two polarizations can degrade the BER. In long transmission systems, these two polarization mix stochastically, so that pulse broadening is not easy to compensate [49]. In a short grating component, however, PMD is not generally large in transmission, since the pulse arrival times are simply due to the difference in the propagation constants of the two polarization states times the length of the grating. In a chirped dispersion compensating reflection grating (DCG), the effect of birefringence is more severe, causing a large additional dispersion. PMD, or more correctly, birefringence induced PMD, in unapodized gratings is more of a nuisance than in unapodized gratings.

In order to assess the impact on the PMD of birefringence in a fiber, whether intrinsic or due to the process of fabrication of a grating, we examine how the Bragg wavelength of a grating is affected by a change

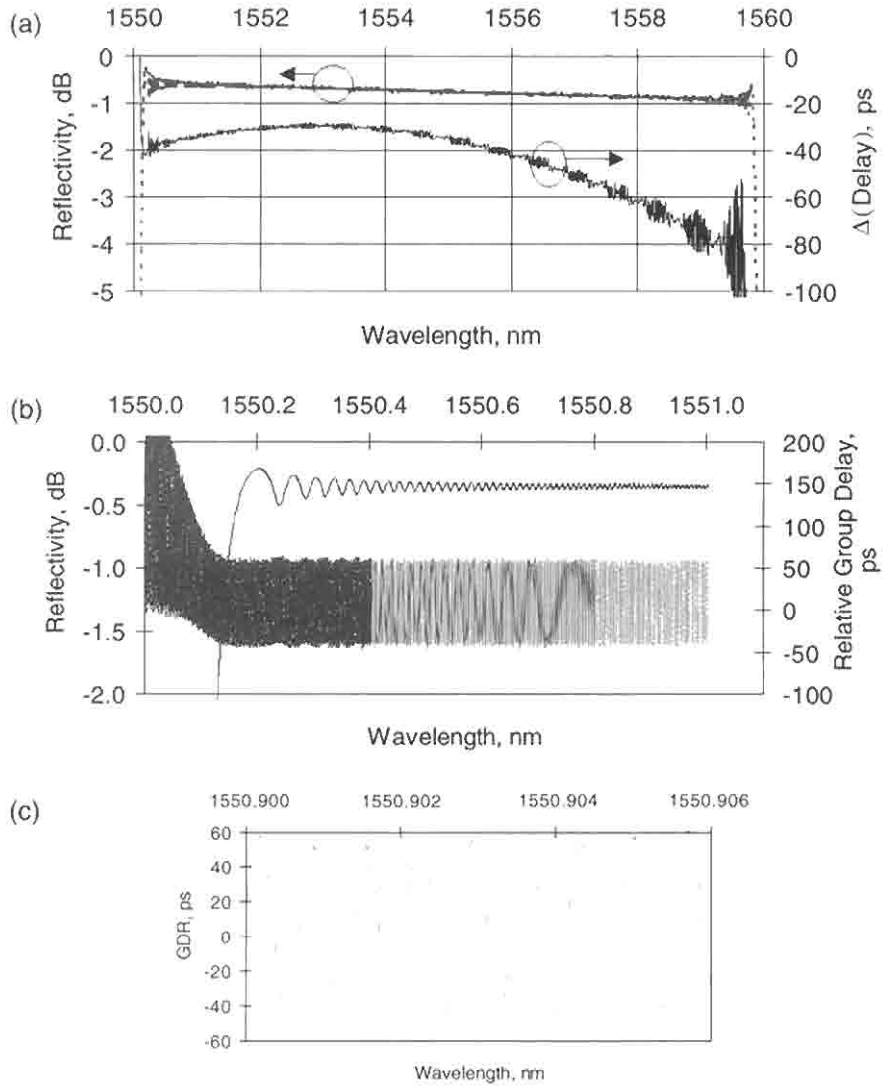

Figure 7.22: (a) The simulated reflectivity and group delay difference form a linear slope of 1310 psec/nm, for a 1.3-m-long SSCG with no stitching errors. (b) High resolution (0.1-pm) simulation of a 1-meter-long grating showing the reflectivity and the group delay ripple. (c) Detail of the relative group delay ripple of (b).

in the effective index of a mode. We assume that the central Bragg wavelength of a chirped grating is

$$\lambda_{Bragg} = 2n_{eff}\Lambda_g, \tag{7.4.1}$$

so that the change in the reflection wavelength as a function of the change in the mode index becomes,

$$\delta\lambda_{Bragg} = \lambda_{Bragg}\frac{\delta n_{eff}}{n_{eff}}. \tag{7.4.2}$$

Equating the change in the mode index to the birefringence in the fiber leads to

$$\delta\lambda_{Bragg} = \lambda_{Bragg}\frac{B}{n_{eff}}. \tag{7.4.3}$$

For a DCG with a dispersion of D_g psec/nm, a change in the Bragg wavelength as a result of the change in the *polarization* induces a delay, $\tau_{PMD} = \delta\lambda_{Bragg}D_g$, from which we get the result

$$\tau_{PMD} = \lambda_{Bragg}B'D_g, \tag{7.4.4}$$

where B' is the normalized birefringence, $\sim B/n_{eff}$. Equation (7.4.4) shows that the PMD is dependent on the dispersion and birefringence but *not* on the length of the grating. A chirped reflection grating with a perfectly linear dispersion of 1310 psec/nm and a birefringence of 10^{-5} at a wavelength of 1550 nm will have a PMD of 28 psec! This result is of the order that has been reported in apodized DCGs [50]. It is clear that even a small birefringence causes a severe PMD penalty. Figure 7.23 shows how the PMD changes with grating dispersion as a function of birefringence. For high dispersion values, it may be impossible to achieve the low birefringence needed for a low PMD value. For example, a dispersion of 5 nsec/nm and a PMD of 1 psec require a birefringence of $\sim 6 \times 10^{-8}$, a value that may not be achievable even with gratings in standard fibers.

The problem is compounded if the DCG is unapodized. From Eq. (7.4.3) we note that the change in the Bragg reflection wavelength is $\sim$0.02 nm for a birefringence of 1×10^{-5} at a wavelength of 1550 nm. Since there is a high-frequency ripple of period $\sim$0.01 nm on the short-wavelength side of the DCG shown in Fig. 7.10, on an overall average dispersion slope of 1310 psec/nm, large jumps in PMD may occur, even with very weak birefringence. These jumps could be of the order of the amplitude of the ripple (100 psec).

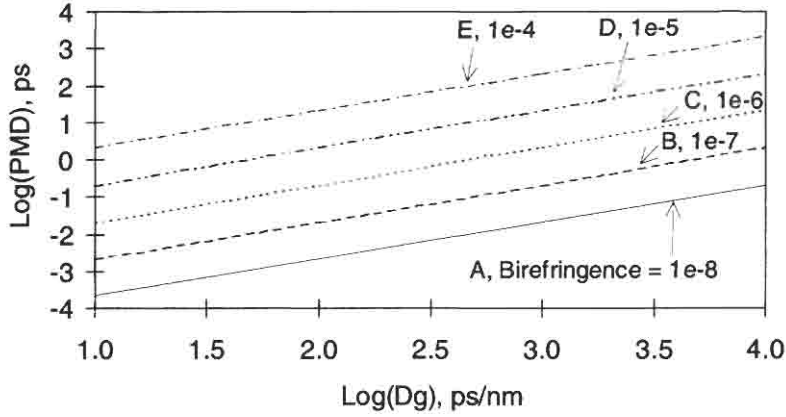

Figure 7.23: PMD vs dispersion in a DCG for five values of birefringence, A ($B = 1 \times 10^{-8}$), B ($B = 1 \times 10^{-7}$), C ($B = 1 \times 10^{-6}$), D ($B = 1 \times 10^{-5}$), and E ($B = 1 \times 10^{-4}$).

7.5 Systems measurements with DCGs

Ultimately, the effectiveness of the DCG is determined by the bit error rate (BER). This measurement is an indicator of the how many errors are received within a certain time window. Generally, a system is expected to achieve a minimum BER of 1 bit in 10^{-9} at the transmission rate, without and with the DCG. Some undersea systems require even lower BERs (e.g., 10^{-15}). However, in order to compare the transmission performance, the power has to be increased at the receiver to compensate for insertion loss and any nonlinear dispersion in the DCG. This is usually expressed as a penalty in decibels at the BER.

There are several parameters that influence the BER. As has been seen, the DCG has an operating bandwidth that needs to accommodate the signal down to −20 dB, to reduce the dispersive effects of spectral filtering. Ideally, a filter matched to the signal bandwidth with perfect dispersion compensation is required with zero insertion loss. Other considerations, such as the effect of different types of apodization on the group delay ripple (GDR) as well as the ripple in the reflected signal of a DCG, PMD, insertion loss, and so on, cause an additional penalty.

There have been many demonstrations of dispersion compensation using DCGs: from compensation of the chirp from a semiconductor laser

using a half-Gaussian refractive index modulation induced chirped grating [2], to the measurement of dispersion in a grating [5], to the first report of DC in a transmission through a fiber [51,52]. In the last demonstration, 400-fsec pulses at a bit rate of 100 Gb/sec was transmitted through 245 m of standard telecommunications fiber and were recompressed with an 8-mm-long 12-nm bandwidth DCG to 450 fsec after dispersing to 30 psec, a compression ratio of ~65. Since these demonstrations many more measurements of DC have been reported using a variety of gratings: notably, dispersion-tunable chirped gratings at 10- and 20-Gb/sec transmission rates with a 5-cm-long grating and 80 km of fiber using strain tuning [53], as well as 220 km at 10 Gb/sec and 100-mm-long temperature-tuned chirped gratings [54]. A novel offset core fiber grating has also been reported for strain tuned dispersion compensation of 270 km of standard fiber at 10 Gb/sec [55,56]. Fixed wavelength, 100-mm-long, chirped gratings have also been used at 10 Gb/sec transmission with up to 500 km of standard fiber [57,11]. Longer gratings, up to 400 mm [58], have been used at 40 Gb/sec over 109 km of fiber, and in excess of 1-m-long gratings with a bandwidth of ~10 nm at 10 Gb/sec over 100 km of standard fiber in a WDM transmission system with up to 11 wavelengths simultaneously [48]. Other WDM experiments at 10 Gb/sec have shown DC at four wavelengths over 100 km using a single superstructure chirped grating (see Chapters 3 and 6) [59].

The long transmission lengths at high bit rates are possible with multiple chirped gratings, either lumped [60,61] or cascaded [12]. In the latter scheme, 8×20 Gb/sec transmission over 315 km used four 1-meter-long continuously chirped gratings at 3×80 km $+ 1 \times 75$ km hops, and 8×10 Gb/sec over 480 km was demonstrated using six 1-meter-long continuously chirped, 6.5-nm bandwidth gratings [62,63] at 80-km hops. The demonstrated results showed near ideal operation at 10 Gb/sec, despite the 4 to 10 psec polarization mode dispersion of each grating, although at 20 Gb/sec there was some polarization dependence. A pseudo random bit sequence of $2^{31} - 1$ was used for the 10 Gb/sec bit stream (and multiplexed for the 20 Gb/sec) for each wavelength spaced at nominally 0.8 nm.

The schemes used for lumped gratings are shown in Fig. 7.24. Either, band-pass filters can be used with identical pairs of gratings as in Fig. 7.24a, or circulators with four or more ports may be used.

Cascading of chirped gratings reduces the available bandwidth and hence system tolerance in multihop routes. This effect is due to filtering

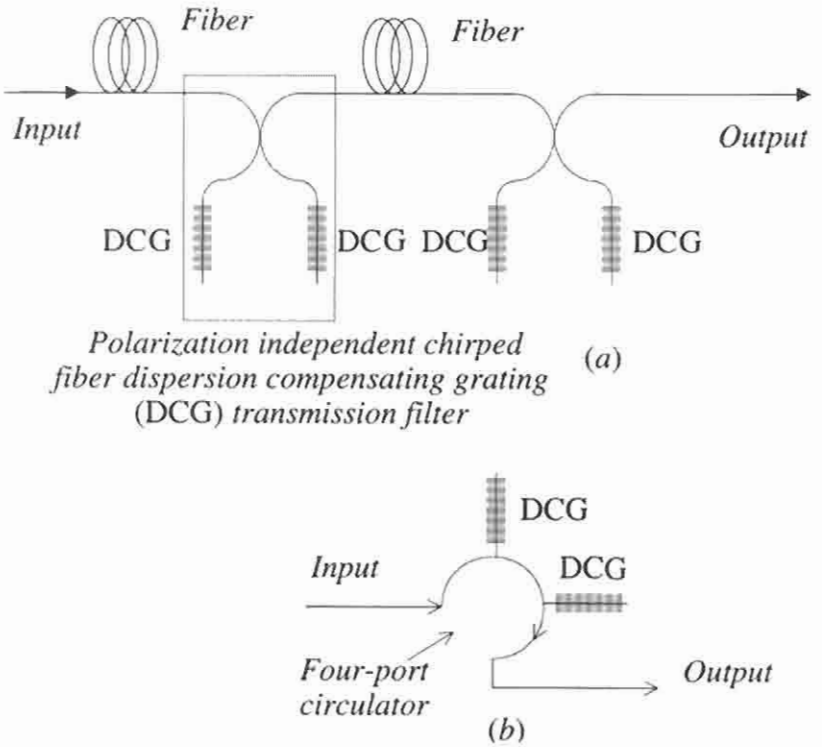

Figure 7.24: The lumped DCG in two configurations: (a) as a band-pass filter (after Ref. [64]) and (b) multiport circulator [65].

at the edges of the grating and is seen clearly in Fig. 7.25. The reflectivity of a cascade of 10 identical hyperbolic-tanh profile gratings shows that the −10 dB (from the peak) signal bandwidth is reduced from 0.8 to 0.6 nm. For this simulation, the reflectivity was ~90% at the peak for the single 100-mm-long grating with a chirped bandwidth (FW) of 0.75 nm. After the tenth reflection the incurred insertion loss was ~5 dB at the peak.

These figures indicate the ideal case for identical gratings. If, however, there is a variation in the bandwidth and the reflectivity, the penalty is worse. For system design, the signal bandwidth determines the bandwidth of the grating. The roll-off of the reflectivity (and therefore the type of apodization) will determine the bandwidth of each grating. Allowance

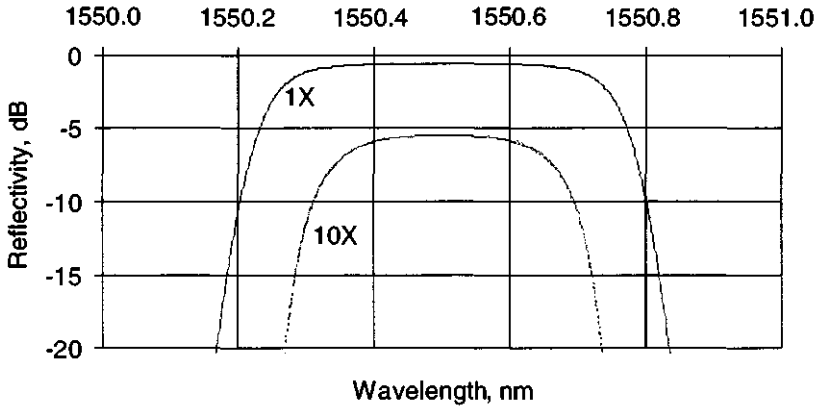

Figure 7.25: The reflectivity of a single and 10 cascaded, 100-mm-long hyperbolic tanh apodized gratings (chirped bandwidth of 0.75 nm and peak–peak refractive index modulation of 7.5×10^{-5}).

also has to be made for drift of the grating wavelengths and the signal source.

For the GDR, cascading of the gratings may have a beneficial effect if the ripple cancels; alternatively, it may increase where it is in phase. This is especially important for unapodized or imperfectly apodized gratings. Some of the large-amplitude high-frequency GDR generated in a cascade of identically apodized gratings is reduced with random variations in the grating profiles. Figure 7.26 shows the relative GDR of a cascade of three identical gratings of type B (in Fig. 7.15) and a for a cascade of all three gratings, B, C, and D.

7.5.1 Systems simulations and chirped grating performance

The theoretical aspects of DCG in systems applications have been considered by the several workers [30,66–70]. Of the many indicators of the performance of a grating, the receiver eye penalty is probably the most significant. As a number alone, it is not very useful, since the properties of the DCG are not constant across the bandwidth. One clearly needs to know the effect of the insertion loss, the change in the reflected power as a function of detuning, and the influence of the nonlinear dispersion.

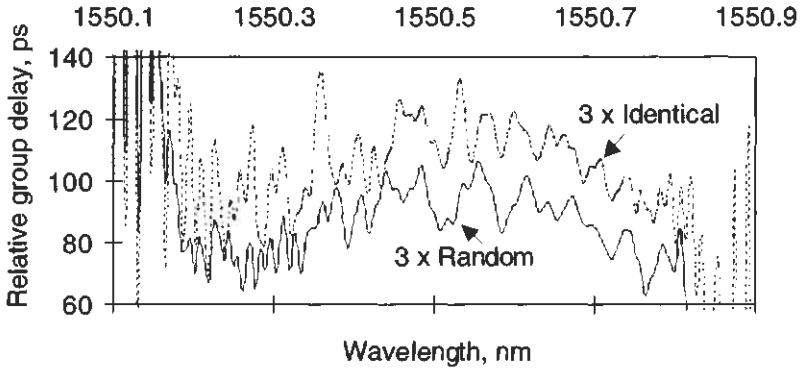

Figure 7.26: Relative GDR for a sequence of three identical chirped gratings of type B in Fig. 7.15, and a mix of types B, C, and D.

Bungarzeanu [71] reported the computer-aided simulation of chirped gratings with a view to understanding the performance of DCGs by comparing the receiver eye closure penalty as a function of detuning across the bandwidth of different apodization profile gratings. This method of analysis is a direct approach to understanding the effect of the group delay ripple, nonlinear dispersion across the bandwidth of the grating, designed for a particular route length. By altering the bit rate, it is possible to map out the point at which the grating will be limited (a) by bandwidth limitation of the grating and (b) by the cumulative effects of the nonlinearity and GDR. The principle of the model is as follows: A 128-bit-long pseudorandom sequence is coded as a non-return-to-zero (NRZ) complex envelope, which is chirp-free. In principle, RZ and chirp may be added. The fiber has a linear dispersion and is a flat-top band-pass filter. The receiver, with a 3-dB bandwidth of 0.75 × bit rate is a fourth-order Bessel-type band-pass filter and is designed to meet the ITU-T guidelines [72]. The time domain output is analyzed and compared with that of an undispersed system to quantify the eye-closure penalty. Figure 7.27 shows the system used for the simulation. It is easy to see how the system can be extended for a more involved simulation.

Figure 7.28a shows the result of the simulations for a transmission over 100 km of standard fiber at a bit rate of 10 Gb/sec, for a 150-mm-long DCG with a dispersion of 1.7 nsec/nm and a FW bandwidth of 107 GHz (0.86 nm). Shown are the results for an unapodized and cosine-and

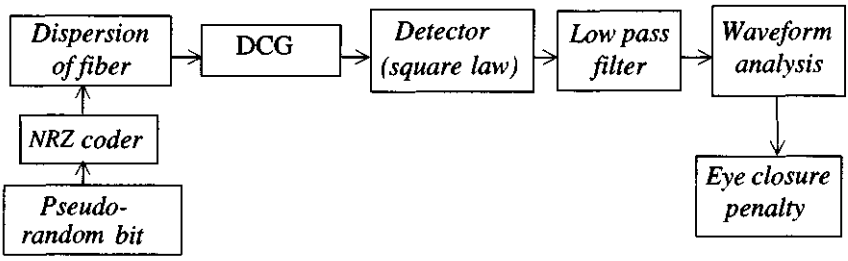

Figure 7.27: The block diagram of the simulation for the calculation of the eye penalty (after ref. [71]).

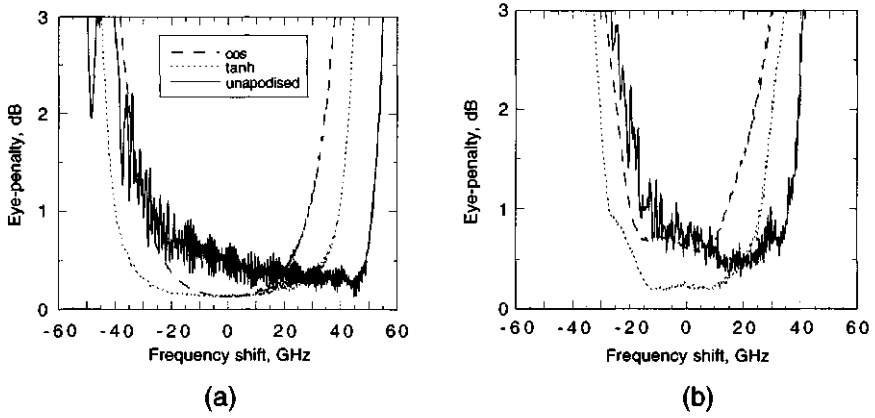

Figure 7.28: The eye-penalty for unapodized and cosine-and tanh-apodized, 150-mm-long gratings for a 10^7-1 NRZ pseudo-random bit sequence, at a bit rate of 10 Gb/sec (a) and 40 Gb/sec (b) (courtesy C. Bungarzeanu [71]).

hyperbolic-tan-apodized profiles as a function of detuning. While the eye penalty is very low (<0.5 dB) close to the short-wavelength end of the unapodized grating, it steadily increases toward the long-wavelength end. Note that the bandwidth is similar to that of the tanh-, but larger than that of the cosine-apodized grating. Also shown in Fig. 7.28b are the simulations for 40 Gb/sec transmission. Here, too, we see that the penalty is only slightly higher than for the tanh-apodized grating (note that the bandwidth for a NRZ is half that of an RZ bit sequence), and the bandwidths are almost identical. Owing to the restricted bandwidth, the detuning is significantly narrower for the cosine-apodized grating.

We note that at the longer-wavelength end of the unapodized grating, the eye penalty fluctuates because of the GDR frequency becoming closer to the transmission frequency, since the eye closes as a result of the additional dispersion. This becomes less important for 40 Gb/sec, since more of the grating bandwidth is being used for dispersion compensation, and the fluctuations on the long-wavelength side also become smaller. This result has been further investigated by Garthe *et al.* [73] for long gratings. The conclusions are similar, in that the eye penalty has a maximum value depending on the position in the bandwidth, because the GDR frequency induces satellite pulses that may coincide with adjacent time slots.

Figure 7.29 shows the reflection and relative group delay of a 200-mm-long SSCG made with two 100-mm-long chirped gratings. Low-repetition-rate ultrahigh-speed measurements performed on this grating with a dispersion of 1310 psec/nm and bandwidth of 1.5 nm at the output of 77 km of standard telecommunications fiber [74] shows that a 3.8 psec input pulse sits on a wide low-level pedestal at the output. The pedestal, which is limited to approximately two bit periods, has the detrimental effect of causing the eye to close slightly when the entire bandwidth of the grating is used. However, systems transmission experiments performed on the same grating at 40 Gb/sec over 77 km of standard fiber indicate that the received eye remains open, as shown in Fig. 7.30, which without the DCG is completely closed.

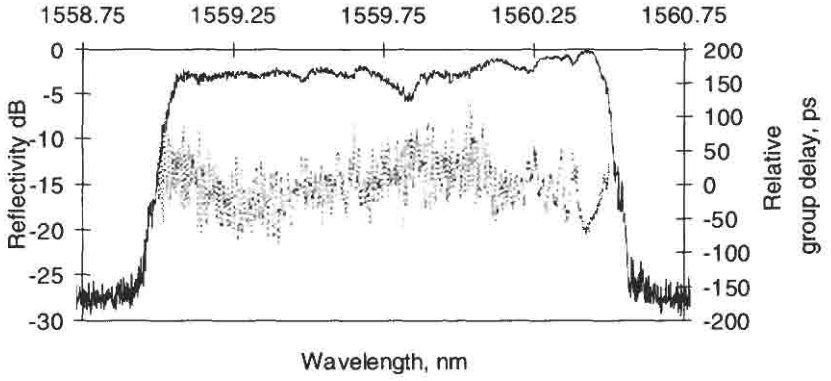

Figure 7.29: The reflectivity and relative group delay of a 200-mm SSCG (dispersion of 1310 psec/nm) [74].

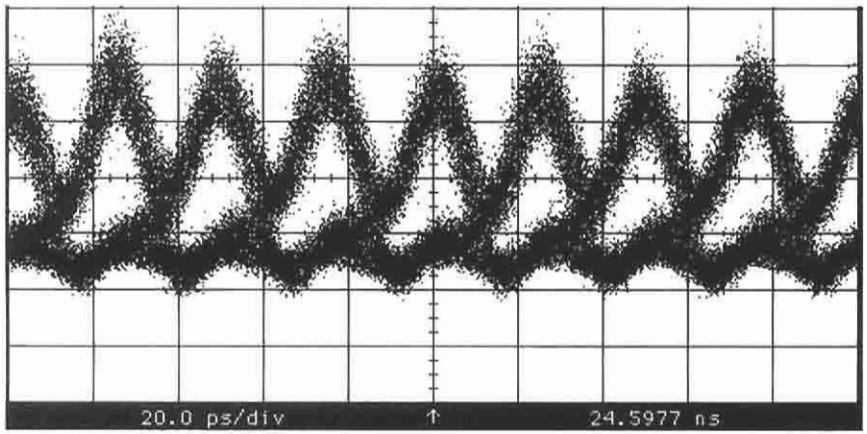

Figure 7.30: The received signal eye diagram at a transmission bit rate of 40 Gb/sec (1550 nm) after 80 km of optical standard fiber and a 200-mm-long unapodized SSCG dispersion compensating grating (courtesy D. Nesset, BT Laboratories).

7.6 Other applications of chirped gratings

As we have seen, pulses propagating in a fiber are broadened by dispersion. There is a broadening if the pulse is not transform limited and it is chirped. Thus, the individual parts of the spectrum arrive at different times and can skew the pulse. If the chirp is a time-varying function, then jitter is also introduced. On the other hand, in a dispersion-free system, neither the chirp introduced by any component nor the source bandwidth causes the pulse to be broadened. If a chirped grating compensates for the dispersion of a fiber, then the dispersion and jitter induced in chirped pulses is automatically compensated [75]. Further, pulses can be compressed or dispersed depending on the sign of the chirp, by launching the pulse in a fiber with either anomalous or normal dispersion. If a pulse is chirped, then it is possible to compensate for the chirp using a chirped fiber grating and to compress the pulse [14,76–80]. The grating may also be used for nonlinear pulse compression [81] of pulses that have been spectrally broadened and linearly chirped through self-phase modulation (SPM) and propagation in normally dispersive optical fiber [82].

For high-power use, chirped gratings are especially suitable for reducing nonlinear effects in the fiber by stretching pulses, reducing the peak power before amplification [13,83].

Adjustment of the chirp of the grating also allows the effects of higher-order dispersion to be canceled [10].

References

1. Byron K. C., Sugden K., Bircheno T., and Bennion I., "Fabrication of chirped Bragg gratings in photosensitive fibre," *Electron. Lett.* **29**(18), 1659 (1993).
2. Eggleton B., Krug P. A., and Poladin L., "Dispersion compensation by using Bragg grating filters with self induced chirp," in *Tech. Digest of Opt. Fib. Comm. Conf., OFC '94,* p. 227.
3. Farries M. C., Sugden K., Reid D. C. J., Bennion I., Molony A., and Goodwin M. J., "Very broad reflection bandwidth (44 nm) chirped fibre gratings and narrow-bandpass filters produced by the use of an amplitude mask," *Electron. Lett.* **30**(11), 891–892 (1994).
4. Ouellette F., "The effect of profile noise on the spectral response of fiber gratings," in *Bragg Gratings, Photosensitivity, and Poling in Glass Fibers and Waveguides: Applications and Fundamentals,* Vol. 17, OSA Technical Digest Series (Optical Society of America, Washington, DC, 1997), paper BMG13, pp. 222–224.
5. Hill K. O., Bilodeau F., Malo B., Kitagawa T., Theriault, Johnson D. C., and Albert J., "Aperiodic in fibre gratings for optical fiber dispersion compensation," in *Technical Digest of Post-Deadline Papers,* PD2-1, *Opt. Fib. Comm. Conf., OFC '94.*
6. Stephens T., Krug P. A., Brodzeli Z., Doshi G., Ouellette F., and Poladin L., "257 km transmission at 10 Gb/s in non dispersion shifted fibre using an unchirped fibre Bragg grating dispersion compensator," *Electron. Lett.* **32**(17), 1559–1561 (1996).
7. Kashyap R., McKee P. F., Campbell R. J., and Williams D. L., "A novel method of writing photo-induced chirped Bragg gratings in optical fibres," *Electron. Lett.* (12), 996–997 (1994).
8. Okude S., Sakai T., Wada A., and Yamauchi R., "Novel chirped fiber grating utilizing a thermally diffused taper-core fiber," in *Proc. of OFC '96,* paper TuO7, pp. 68–69.

9. Putnam M. A., Williams G. M., and Friebele E. J., " 'Fabrication of tapered, strain-gradient chirped fibre Bragg gratings," *Electron. Lett.* **31**(4), 309–310 (1995).

10. Laming R. I., Ibsen M., Durkin M., Cole M. J., Zervas M. N., Ennser K. E., and Gusmeroli V., "Dispersion compensation gratings," in *Bragg Gratings, Photosensivity, and Poling in Glass Fibers and Waveguides: Applications and Fundamentals,* Vol. 17, OSA Technical Digest Series (Optical Society of America, Washington, DC, 1997), Paper BTuA7, pp. 271–273.

11. Loh W. H., Laming R. I., Robinson N., Cavaciuti A., Vaninetti, Anderson C. J., Zervas M. N., and Cole M. J., "Dispersion compensation over distances in excess of 500 km for 10 Gb/s systems using chirped fibre gratings," *IEEE Photon. Technol. Lett.* **8**, 944 (1996).

12. Garrett L. D., Gnauck A. H., Forgherieri, and Scarano D., "8 × 20 Gb/s–315 km–480 km WDM transmission over conventional fiber using multiple broadband fiber gratings," in *Tech. Digest of Conf. On Opt. Fiber Commun., OFC '98,* Post-Deadline paper, PD18/1–4.

13. Boskovic A., Guy M. J., Chernikov S. V., Taylor J. R., and Kashyap R., "All-fiber diode pumped, femtosecond chirped pulse amplification system," *Electron. Lett.* **31**(11), 877–879 (1995).

14. Gunning P., Kashyap R., Siddiqui A. S., and Smith K., "Picosecond pulse generation of <5 ps from gain-switched DFB semiconductor laser diode using linearly step-chirped fibre grating," *Electron. Lett.* **31**(13), 1066–1067 (1995).

15. Kersey A. D. and Davis M. A., "Interferometric fiber sensor with a chirped grating distributed sensor element," *Proc. OFS '94,* pp. 319–322, Glasgow, UK (1994).

16. Williams J. A. R., Bennion I., and Doran N. J. "The design of in-fiber Bragg grating systems for cubic and quadratic dispersion compensation," *Opt. Commun.,* **116**(1–3), 62–66 (1995).

17. Farries M. C., Ragdale G. M., and Reid D. C. J., "Broadband chirped fiber Bragg grating filters for pump rejection and recycling in erbium doped fibre amplifiers," *Electron. Lett.,* 28, 487–489 (1992).

18. Kashyap R., Wyatt R., and McKee P. F., "Wavelength flattened saturated erbium amplifier using multiple side-tap Bragg gratings," *Electron. Lett.* **29**(11), 1025 (1993).

19. Zhang I., Sugden K., Williams J. A. R., and Bennion I., "Postfabrication exposure of gap-type bandpass filters in broadly chirped fiber gratings," *Opt. Lett.* **20**(18), 1927–1929 (1995).

20. Treacy E. B., "Optical pulse compression with diffraction gratings," *Quantum Electron.* **QE-5**, 454 (1969).

21. Nakatsuka H., Grischkowsky D., and Balant A. C., "Nonlinear picosecond pulse propagation through optical fibers with positive group velocity dispersion," *Phys. Rev. Lett.* **47**, 910 (1981).

22. Shank C. V., Fork R. L., Yen R., Stolen R. H., and Tomlinson W. J., *Appl. Phys. Lett.* **40**, 761 (1982).

23. Winful H. G., "Pulse compression in optical fiber filters," *Appl. Phys. Lett.* **46**(6), 527 (1985).

24. See, for example, Sterke C. M. de, and Sipe J. E., "Gap solitons," in *Progress in Optics XXXIII* (E. Wolf, Ed.), Chapter III. Elsevier, Amsterdam (1994).

25. Eggleton B. J., Slusher R. E., Strasser T. A. and Sterke M. de, "High intensity pulse propagation in fiber Bragg gratings," in *Bragg Gratings, Photosensitivity, and Poling in Glass Fibers and Waveguides: Applications and Fundamentals,* Vol. 17, OSA Technical Digest Series (Optical Society of America, Washington, DC, 1997), Paper BMB1, pp. 114–116.

26. Chen L. R., Benjamin S. D., Smith P. W. E., and Sipe J. E., "Ultrashort pulse propagation through fiber gratings: Theory and experiment," *ibid.,* paper BMB2, pp. 117–119.

27. Taverner D., Broderick N. G. R., Richardson D. J., and Ibsen M., "Nonlinear switching and multiple gap soliton formation in a fibre Bragg grating," *ibid.,* paper BMB3, pp. 120–123.

28. Broderick N. G. R., Taverner D., Richardson D. J., Ibsen M., and Laming R. I., "The optical pushbroom in action" *ibid.,* paper BMB4, pp. 123–125.

29. Kuo C. P., Österberg U., Seaton C. T., Stegeman G. I., and Hill K. O., "Optical fibers with negative group-velocity dispersion in the visible," *Opt. Lett.* **13**(11), 1032–1034 (1988).

30. Ouellette F., "Limits of chirped pulse compression with an unchirped Bragg grating filter," *Appl. Opt.* **29**(32), 4826 (1990).

31. Eggleton B. J., Stephens T., Krug P. A., Doshi G., Brodzeli Z., and Ouellette F., "Dispersion compensation over 100 km at 10 Gb/sec using a Bragg grating in transmission," in *Tech. Digest. of OFC '96,* post-deadline paper PD5 (1–5).

32. Litchinistser N. M., Eggleton B. J., and Patterson D. B., "Fiber Bragg gratings for dispersion compensation in transmission: theoretical model and design criteria for nearly ideal pulse recompression," *J. Lightwave Technol.* **15**(8), 1301–1313 (1997).

33. Hinton K., "Ramped, unchirped fiber gratings for dispersion compensation," *J. Lightwave Technol.* **15**(8), 1141–1418 (1997).

34. Ouellette F., "Dispersion cancellation using linearly chirped Bragg grating filters in optical waveguides," *Opt. Lett.* **12**(10), 847 (1987).

35. Priest R. G. and Giallorenzi T. G., "Dispersion compensation in coherent fiber-optic communications," *Opt. Lett.* **12**, 622–625 (1987).

36. Boness R., Nowak W., Vobian J., Unger S., and Kirchoff J., "Tailoring of dispersion compensation fibers with high compensation ratios up to 30," *Pure Appl. Opt.*, **5**, 333 (1995).

37. Agrawal G. P., *Nonlinear Fiber Optics,* 2nd ed. Academic Press, New York (1995).

38. Marcuse D., *Appl. Opt.* **19**, 1563 (1980).

39. Kashyap R., "Design of step chirped gratings," *Optics Commun.* **136**(5,6), 461–469 (1997).

40. Boskovic A., Taylor J. R., and Kashyap R., "Forty times dispersive broadening femtosecond pulses and complete recompression in a chirped fibre grating," *Opts. Commun.* **119**, 51–55 (1995).

41. Bonino S., Norgia M., and Riccardi E., "Spectral behaviour analysis of chirped fibre Bragg gratings for optical dispersion compensation," in *Proc. of ECOC '97, IEE Conf. Pub. No. 448,* Vol.3, pp. 194–197.

42. Kashyap R. and Lacerda-Rocha M. de, "On the group delay of chirped fibre Bragg gratings," *Opt. Commun.* **153**, 19–22 (1998).

43. Hill K. O., Thériault S., Malo B., Bilodeau F., Kitagawa T., Johnson D. C., Albert J., Takiguchi T., Kataoka T., and Hagimoto K., "Chirped in-fibre grating dispersion compensators: Linearisation of dispersion characteristic and demonstration of dispersion compensation in 100 km, 10 Gbit/s optical fibre link," *Electron. Lett.* **30**(21), 1755–1756 (1994).

44. Roman J. E. and Winnick K. A., "Waveguide grating filters for dispersion compensation and pulse compression," *IEEE J Quantum Electron* **29**(3), 975 (1993).

45. Arkwright J., Stephens T., Stepanov D. Yu, Krug P., Smith B., Doshi G., Joffe G., and Ouellette F., "Fibre gratings for dispersion compensation," in *Proc. of ECOC '97, IEE Conf. Pub. No. 448* (1997).

46. Kashyap R., Froehlich H-G., Swanton A., and Armes D. J., "Super-step-chirped fibre Bragg gratings," *Electron. Lett.* **32**(15), 1394–1396 (1996).

47. Kashyap R., Froehlich H-G., Swanton A., and Armes D. J., "1.3 m long super-step-chirped fibre Bragg grating with a continuous delay of 13.5 ns and bandwidth 10 nm for broadband dispersion compensation," *Electron. Lett.* **32**(19), 1807–1809 (1996).

48. Kashyap R., Ellis A., Malyon D., Froehlich H-G., Swanton A., and Armes D. J., "Eight wavelength × 10Gb/s simultaneous dispersion compensation over 100 km singlemode fibre using a single 10 nm bandwidth, 1.3 metre long, super-step-chirped fibre Bragg grating a continuous delay of 13.5 ns,"

in *Proc. of Post Deadline Papers of the 22nd ECOC '97,* Oslo, Norway, Sept. 15–19 (1996).

49. Curti F., Diano B., Marchis G. C., and Matera F., "Statistical treatment of the principal states of polarization in single-mode fibers," *J. Lightwave Technol.,* **8**(8), 1162–1166 (1990).

50. Bonino S., Norgia M., Riccardi E., and Schiano M., "Measurement of polarisation properties of chirped fibre gratings," in *Technical Digest of OFMC '97,* pp. 10–13.

51. Kashyap R., Chernikov S. V., McKee P. F., and Taylor J. R., "30 *ps* chromatic dispersion compensation of 400 *fs* pulses at 100 *Gbit/s* using an all fibre photoinduced chirped reflection grating," *Electron. Lett.* **30**(13), 1078 (1994).

52. Kashyap R., Chernikov S. V., McKee P. F., Williams D. L., and Taylor J. R., "Demonstration of dispersion compensation in all-fibre photoinduced chirped gratings," *Pure Appl. Opt.* **4**, 425–429 (1995).

53. Garthe D., Lee W. S., Epworth R. E., Bircheno T., and Chew C. P., "Practical dispersion equaliser based on fibre gratings with a bitrate length product of 1.6 Tb/s-km," post-deadline paper, in *Technical Digest of ECOC '94,* pp. 11–14.

54. Laming R. I., Robinson N., Scrivener P. L., Zervas M. N., Barcelos S., Reekie L., and Trucknott J. A., "Dispersion tunable grating in a 10-Gb/s 100–220 km step-index fiber link," *IEEE Photon. Technol. Lett.* **8**(3), 428–430 (1996).

55. Krug P. A., Stephens T., Yoffe G., Ouellette F., Hill P., and Doshi G., "270 km transmission at 10 Gb/s in nondispersion shifted fiber using an adjustably chirped 120 mm long fiber Bragg grating dispersion compensator," in *Tech. Digest of Conf. on Opt. Fiber Commun., OFC '95,* post-deadline paper PDP27.

56. Krug P. A., Stephens T., Yoffe G., Ouellette F., Hill P., and Doshi G., "Dispersion compensation over 270 km at 10 Gb/s using an offset-core fibre Bragg grating," *Electron. Lett.* **19**, 877–879 (1994).

57. Loh W. H., Laming R. I., Gu X., Zervas M. N., Cole M. J., Widdowson T., and Ellis A. D., "10 cm chirped fibre Bragg grating for dispersion compensation at 10 Gb/s over 400 km of non-dispersion shifted fibre," *Electron. Lett.* **31**(25), 2203–2204 (1995).

58. Dong L., Cole M. J., Ellis A. D., Durkin M., Ibsen, Gusmeroli V., and Laming R. I., "40 Gb/s 1.55 μm transmission over 109 km of non-dispersion shifted fibre with long continuously chirped gratings," in *Tech. Digest of Conf. on Opt. Fiber Commun., OFC '97,* post-deadline paper PD6.

59. Ouellette F., Krug P. A., Stephens T., Doshi G., and Eggleton B., "Broadband and WDM dispersion compensation using chirped sampled fibre Bragg gratings," *Electron. Lett.* **3**(11), 899–901 (1995).

60. Chernikov S. V., Kashyap R., and Taylor J. R., "Dispersion compensation of a 100-Gb/s optical fibre transmission by using a chirped fibre grating transmission filter," *Tech. Digest of Conf. on Opt. Fiber Commun., OFC '95,* paper WB5, pp. 99–100.

61. Taverner D., Richardson D. J., Barcelos S., Zervas M. N., Reekie L., and Laming R. I., "Dispersion compensation of 16 ps pulses over 100 km of step-index fibre using cascaded chirped fibre gratings," *Electron. Lett.* **31**(12), 1004–1006 (1995).

62. Cole M. J., Geiger H., Laming R. I., Zervas M. N., Loh W. H., and Gusmeroli V., "Broadband dispersion compensation chirped fibre Bragg gratings in a 10 Gb/s NRZ 110 km standard step index monomode fibre link," *Electron. Lett.* **33**(1), 70–71 (1997).

63. Dong L., Cole M. J., Ellis A. D., Durkin M., Ibsen M., Gusmeroli V., and Laming R. I., "40 Gb/s 1.55 μm RZ transmission over 109 km of non-dispersion shifted fiber with long continuously chirped fibre gratings," *Electron Lett,* **33**, 1563–1565 (1997).

64. Chernikov S. V., Taylor J. R., and Kashyap R., "All-fiber dispersive transmission filters based on fiber grating reflectors," *Opt. Lett.* **20**(14), 1586–1588 (1995).

65. Huber D. R., "Erbium doped amplifier with a 21 GHz optical filter based on an in-fiber Bragg grating," in *Proc. of ECOC '92,* pp. 473–476 (1992).

66. Ouellette F., Cliche M., and Gagnon S., "All-fiber devices for chromatic dispersion compensation based on chirped distributed resonant coupling," *J. Lightwave Technol.* **12**(10), 1728–1737 (1994).

67. Mason P. L., Penty R. V., and White I. H., "Multiple stage dispersion compensation in long haul optical fibre systems using chirped fibre Bragg gratings," *Electron. Lett.* **30**(15), 1244–1245 (1994).

68. Pastor D., Capmany J., Ortega D., Tatay V., and Marti J., "Design of apodized linearly chirped fiber gratings for dispersion compensation," *J. Lightwave Technol.* **14**(11), 2581–2588 (1996).

69. Litchinitser N., and Patterson D., "Analysis of fiber Bragg gratings for dispersion compensation in reflective and transmissive geometries," *J. Lightwave Technol.* **15**(8), 1323–1328 (1997).

70. Ennser K., Zervas M. N., and Laming R. I., "Optimization of linearly chirped grating dispersion compensated system," *Opt. Fiber Technol.* **3**, 120–122 (1997).

71. Bungarzeanu C., "Computer aided design of linearly chirped fibre gratings used as broadband dispersion compensators," in *Proc. of ITA–Information,*

Telecommunications, Automata Journal, Vol. 15, No. 1–3, 1997, ISSN 0351-7748.

72. *International Telecommunications Union-T, Recommendation G. 957.*
73. Garthe D., Milner G., and Cai Y., "System performance of broadband dispersion compensating gratings," *Electron. Lett.* **34**(6), 582–583 (1998).
74. Guy M. J., Taylor J. R., and Kashyap R., "Demonstration of the possibility of >100 Gbit/s transmission over 77 km of standard fibre using a super-step-chirped fibre grating dispersion compensator," *Opt. Commun.* **150**, 77–80 (1998).
75. Kawase L., Carvalho M. C. R., Margulis, and Kashyap R., "Transmission of chirped optical pulses in fibre grating dispersion compensated system," *Electron. Lett.* **33**(2), 152–154 (1997).
76. Eggleton B. J., Krug P. A., Poladin L., Ahmed K. A., and Liu J-F, "Experimental demonstration of compression of dispersed optical pulses by reflection from a self-chirped optical fiber Bragg gratings," *Opt. Lett.* **19**, 877–879 (1994).
77. Rottwitt K., Guy M. J., Boskovic A., Noske D. U., Taylor J. R., and Kashyap R., "Interaction of uniform phase picosecond pulses with chirped and unchirped photosensitive fibre Bragg gratings," *Electron. Lett.* **30**(12), 995–996 (1994).
78. Pataca D. M., Rocha M. L., Kashyap R., and Smith K., "Bright and dark pulse generation in an optically mode-locked fibre laser at 1.3 μm," *Electron. Lett.* **31**(1), 35–36 (1995).
79. Guy M. J., Chernikov S. V., Taylor J. R., Moodie D. G., and Kashyap R., "Generation of transform limited optical pulses at 10 GHz using an electro-absorption modulator and a chirped fibre Bragg grating," *Electron. Lett.* **31**(8), 671–672 (1995).
80. Morton P. A., Mizrahi V., Kosinski S. G., Mollenauer L. F., Tanbun-Ek T., Logan R. A., Coblentz D. L., Sargent A. M., and Wecht K. W., "Hybrid soliton pulse source with fibre external cavity and Bragg reflector," *Electron. Lett.* **28**(6), 561 (1992).
81. Williams J. A. R., Bennion I., and Zhang L., "The compression of optical pulses using self-phase modulation and linearly chirped Bragg gratings in fibers," *IEEE Photon. Technol. Lett.* **7**(5), 491–493 (1995).
82. Tomlinson W. J., Stolen R. H., and Shank C. V., "Compression of pulses chirped by self-phase modulation in fibers," *J. Opt. Soc. Am. B* **1**, 139–149 (1984).
83. Galvanauskas A., Fermann M. E., Harter D., Sugden K., and Bennion I., "All-fiber femtosecond pulse amplification circuit using chirped Bragg gratings," *Appl. Phys. Lett.* **66**, 1053–1055 (1995).

This page intentionally left blank